NUNAVIK AND NUNATSIAVUT REGIONAL CLIMATE INFORMATION UPDATE

LEAD AUTHORS: Carl Barrette, Ross Brown and Robert Way

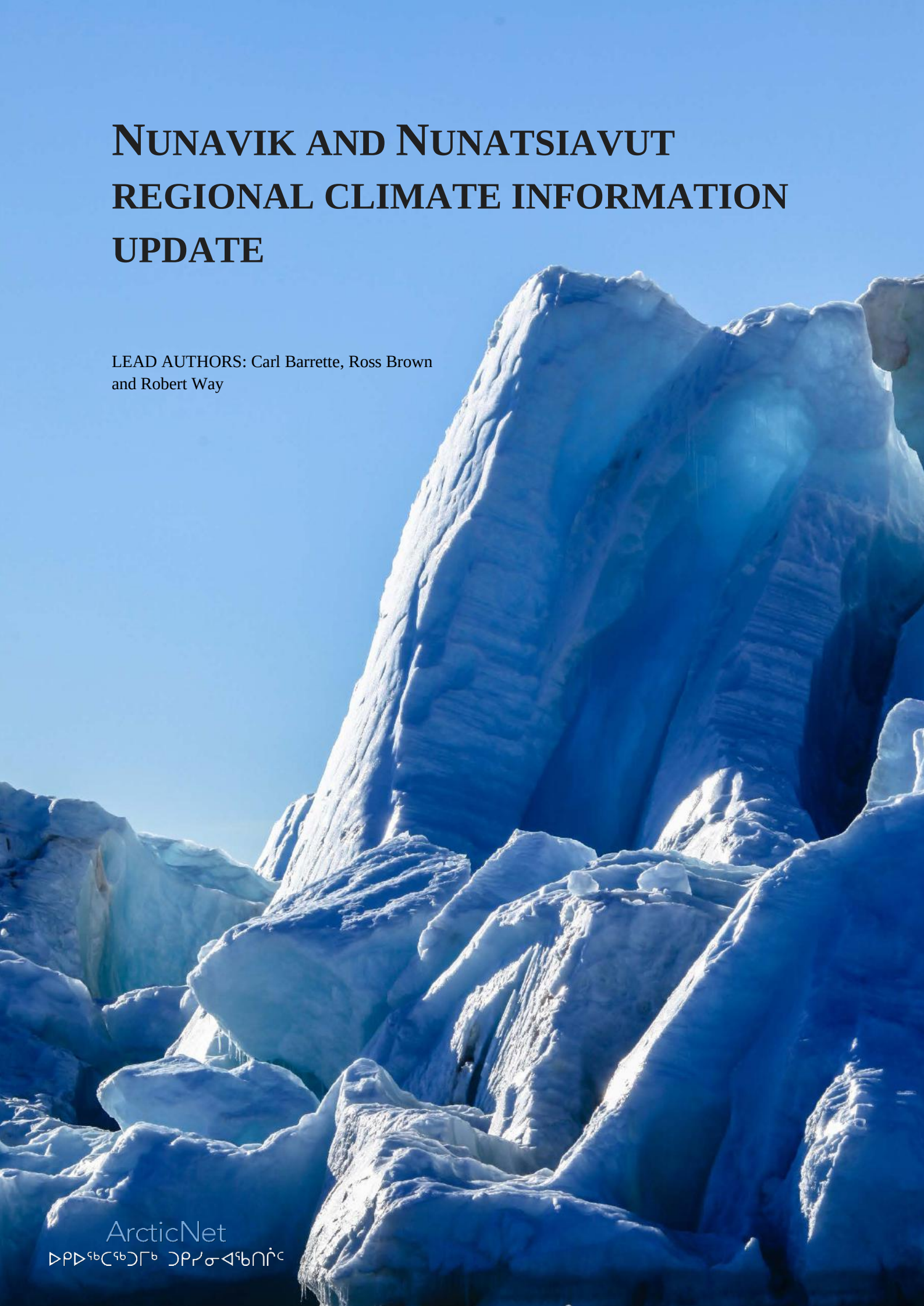

ArcticNet
ᐅᑭᐅᖅᑕᖅᑐᑦ ᑐᑭᓯᓂᐊᖅᑎᑦᑕ

NUNAVIK AND NUNATSIAVUT REGIONAL CLIMATE INFORMATION UPDATE

Lead authors: Carl Barrette, Ross Brown and Robert Way

Contributing authors: Alain Mailhot, Émilia Paula Diaconescu, Patrick Grenier, Diane Chaumont, Dany Dumont, Caroline Sévigny, Stephen Howell, Simon Senneville

This document should be cited as:

Barrette C, Brown R, Way R, Mailhot A, Diaconescu EP, Grenier P, Chaumont D, Dumont D, Sévigny C, Howell S, Senneville S. 2020. Chapter 2: Nunavik and Nunatsiavut regional climate information update. In Ropars P, Allard M, Lemay M (eds.), Nunavik and Nunatsiavut: From science to policy, an integrated regional impact study (IRIS) of climate change and modernization, second iteration. ArcticNet Inc, Québec, Canada.

ArcticNet
ᐅᑭᐅᖅᑕᖅᑐᒃ ᑐᑭᓯᓂᐊᖅᑎᑦᑕ

OURANOS

Queen's University

Environment and Climate Change Canada
Environnement et Changement climatique Canada

Key messages

- **Climate observations and local knowledge provide largely consistent evidence of important changes in air temperature, precipitation, snow cover, wind, lake ice and coastal sea-ice over Nunavik and Nunatsiavut.** The surface air temperature observing network shows that the Nunavik and Nunatsiavut region is continuing to experience increasing temperatures with the 1987–2016 period characterized by pronounced winter warming up to 2.0 °C/decade over northernmost areas which is consistent with poleward amplification of global warming. The region has also experienced widespread summer warming of ~0.5 °C/decade. These warming trends are driving significant cryospheric and environmental changes. Future scenarios show warming trends with mean annual air temperatures increasing by ~2–8 °C by the end of the century. The largest changes (~3–13 °C) are projected for winter months.
- **There is greater uncertainty in observed mean annual precipitation trends, but there is a consensus of a long-term increase of ~ 3 %/decade since the 1950s over the region.** Recent warming is estimated to have contributed to a 13 % decline in the solid fraction of total precipitation over 1980–2014. Mean annual precipitation is projected to increase ~20–35 % by the end of this century.
- **The impact of warming on the duration of the period with freezing temperatures and the fraction of precipitation falling as snow is contributing to a significant decline in the number of days with snow on the ground (~-40 days) and a reduction in maximum snow depth by ~25 cm since the late-1950s.** However, there is greater local and regional variability in observed snow depth trends compared to snow cover duration trends. Declining snow cover trends are projected to persist in the future in response to warming with a projected reduction ranging between ~15–70 days in annual snow cover duration by the end of the century over the region. Maximum snow depth is also projected to decrease substantially over the coastal areas of Nunatsiavut by the end of the century but projected changes in snow depth are less certain over Nunavik.
- **There is relatively little long-term monitoring data for lake and river ice cover in the region but the available observations and community knowledge indicate a widespread trend for earlier ice break-up.** Community-based monitoring of the period that ice is safe to travel at Mud Lake, NL just south of Nunatsiavut shows evidence of a significant (0.05 confidence level) decrease in the period of ice safe for travel of ~4 days/decade since the mid-1970s, with duration closely linked to mean winter air temperatures. Further declines in ice cover duration and stability are expected in response to projected warming.
- **Glaciers in the Torngat Mountains of northern Labrador continue to undergo substantial thinning and retreat since the 1950s in response to warming temperatures.** This trend is expected to continue in the future although the rate may decrease as glaciers retreat deeper into shaded cirque backwalls.

- **Shipping season (summer) ice cover has declined by ~30 %/decade in coastal waters of Nunatsiavut and Hudson Strait-Ungava Bay since 1971.** These decreases are the largest observed in Canadian waters. There is no evidence of any change in shipping season sea ice cover in Hudson Bay. The ice-free period is projected to increase by 90–120 days by the end of the century in response to warming with stronger reductions shown in several locations (e.g., In Hudson Strait near Salluit and Deception Bay as well as in Hudson Bay near the Nastapoka Islands).
- **Model analysis of the coastal ice formation and dynamics show that the period over which ice is safe for travel is highly sensitive to future greenhouse gas emissions.** The safe period is projected to decrease by ~30 days for 2050, but by more than 100 days by the end of the century. The projected reductions are largest along the Hudson Bay coast of Nunavik.
- **Annual maximum air temperatures are projected to increase by ~2 and 4° C respectively for 2050 and 2085 under scenario RCP 8.5.** However, these changes are less rapid than projected increases in mean annual air temperature for the same time periods (~4 and 6° C). Projected warming of cold extremes are contributing most to the mean annual air temperature warming with the largest warming projected in annual minimum daily temperatures (~7 and 15 °C) and extreme cold nights (~6 and 13 °C).
- **Precipitation extremes are projected to increase over the region by ~5 to 10 mm/day respectively for the 2050 and 2085 periods under emission scenario RCP 8.5,** with changes in extreme precipitation systematically stronger than the changes in mean annual precipitation.

1. Introduction

In northern and Arctic regions, climate is one of the primary drivers of change in physical environments and has a clear influence on socio-economic and cultural legacies. Recent regional and pan-arctic assessment reports AMAP (2017a, b, c, d) and Bell and Brown (2018) have documented widespread environmental changes to terrestrial (e.g., permafrost, vegetation, snow cover, lake, and river ice) and marine environments (e.g., sea-ice and fast ice, sea level, and ocean currents, salinity, and mixing layers) over the past several decades. There is also growing evidence that changes related to landscape, vegetation and permafrost over Nunavik and Nunatsiavut, northern Canada, are closely linked to climate changes (Angers-Blondin and Boudreau, 2017; Rapinsky et al., 2017; Way and Lewkowicz, 2016; Bouchard et al., 2014; Fraser et al., 2011).

These changes influence primary productivity, marine and terrestrial wildlife dynamics, trophic chains, water quality and chemistry, and the dispersion and transmission of new or current parasite infections or diseases. The cumulative effects of these widespread environmental changes also negatively impact livelihoods, physical and mental health, well-being, culture and the economy of northern societies (Cunsolo Willox et al., 2015; Pearce et al., 2015; Ford et al., 2013), so that the projected acceleration of Arctic environmental changes over the next century will increasingly apply pressure on natural and human systems to adapt. Amongst the key areas of concern are the availability and quality of country foods (Rosol et al., 2016; Harper et al., 2015) and water quality issues in permafrost dominated regions (Jolivel and Allard, 2017; Deshpande et al., 2015). But not all impacts are negative (Ford et al., 2013). Some changes, such as an extended ice-free navigation period could provide enhanced economic activities (Prowse et al., 2009). A recent study in Nunavik also showed that projected warming may enhance groundwater availability and consequently increase the rate of recharge of the aquifers in the future to the benefit of local communities (Lemieux et al., 2016).

The main objectives of this update are:

(1) to provide a brief overview of the main large scale and local scale climate drivers of change in Nunavik and Nunatsiavut taking into account the new information (Tables A-1 to A-3 in Appendix A) and datasets acquired since the first iteration of the IRIS-4 report (Allard and Lemay, 2012);
(2) to provide a more in-depth focus on the coastal climate where most communities are located;
(3) to present an update of climate variability and trends, and a reference climate for Nunavik and Nunatsiavut based on new data sources and climate information (Diaconescu et al., 2017);
(4) to present key baseline climate indices as well as climate extremes indices that are more relevant to local needs; and
(5) to present climate change projections using time series and maps for the near- and long-term future based on regional downscaling of climate simulations from the North America CORDEX ensemble (Mearns et al., 2017) and CRCM5 regional climate model (Martynov et al., 2013) simulations produced by Ouranos Consortium.

The update is organized into three main sections. The first section presents a brief discussion of the processes influencing the natural climate variability of the region, along with a discussion of key features of the projected changes such as the potential for abrupt cooling events linked to a slowdown of northward heat transport in the Atlantic Ocean in response to freshening of water (Sgubin et al., 2017; Rahmstorf et al., 2015). The second section examines climate variability and trends in the recent past period (~1950–2017) and presents projected changes for two future periods (2046–2064 and 2076–2100) for a range of climate indices linked to air temperature, precipitation, snow cover, wind speed, wave height, and sea-ice. A final summary and conclusions section presents a synthesis of the update material, key conclusions, and recommendations for future work.

2. Climate drivers

2.1 Atmospheric-cryospheric-oceanic influences on climate variability in Nunavik and Nunatsiavut

The climate of Nunavik and Nunatsiavut is strongly influenced by natural variability and quasi-oscillatory behavior in the coupled atmosphere-ocean system with climate impacts on time-scales ranging from years to decades (Allard and Lemay, 2012, section 2.3.6). In this context, evidence of long-term warming can be difficult to disentangle from natural variability over short time periods (Vincent et al., 2015; Way and Viau, 2014). However, several new climate reconstructions for northeastern Canada using tree rings and sediment cores (Richerol et al., 2016; Naulier et al., 2015) have shown that the rates of change over the past few decades are possibly unprecedented over the past millennium.

Principal component and correlation analysis of gridded monthly air temperatures for Labrador and northern Québec (Way et al., 2017) were used to identify the regional influences of atmospheric and oceanic variability. This analysis revealed the presence of three important drivers of the observed variability over Nunavik and Nunatsiavut (Figure 1):

(1) the East Pacific-North Pacific (EP-NP) pattern influence on temperatures over the southwestern part of the region in spring-summer-fall;
(2) the North Atlantic Oscillation and Arctic Oscillations (NAO-AO) influence on winter temperatures (and precipitation) over Nunatsiavut and northern Nunavik; and
(3) the sea surface temperature variability in the northwest Atlantic represented by the Atlantic Multidecadal Oscillation (AMO) that influences summer-fall temperatures over much of Labrador and the Québec North Shore and southern Nunatsiavut.

The EP-NP atmospheric pattern reflects shifts in the location and intensity of the Pacific jet stream which affects cyclonic circulation over eastern North America.

The positive (negative) phase of the EP-NP is associated with cold (warm) temperature anomalies over the southwestern region and has an important influence on the onset and melt of snow cover (Brown et al., 2010). The NAO-AO refers to well-documented interconnected oscillations in the air pressure gradients over the Arctic and northwest Atlantic that influences temperature and precipitation over large regions of Europe and eastern North America (Hurrel, 2013; Thompson and Wallace, 1998). Finally, AMO describes quasi-periodic large-scale sea surface temperature fluctuations over the North Atlantic basin on multi-decadal time scales which has been linked to regional and to global-scale influences on climate (Ruprich-Robert et al., 2017; Trenberth et al., 2007). During fall and spring periods, the AMO and EP-NP are strongly correlated and have effects on the regional temperature variability as shown in Figure 1. In the 2013–2016 period, the NAO contributed to colder than average winter temperatures (Figure 2).

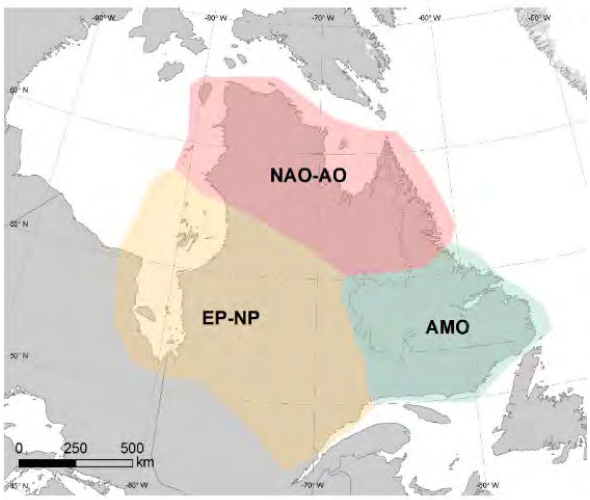

Figure 1: Zones where air temperature is primarily influenced by atmospheric and oceanic teleconnections. The analysis uses monthly AMO, AO, EP-NP and NAO-AO indices from the Climate Prediction Center with leading modes of monthly temperature variability obtained from principal component and correlation analysis of the Way et al. (2017) dataset for Labrador and northern Québec, Canada. Note that the zones represent the average areas of influence which can vary from year-to-year.

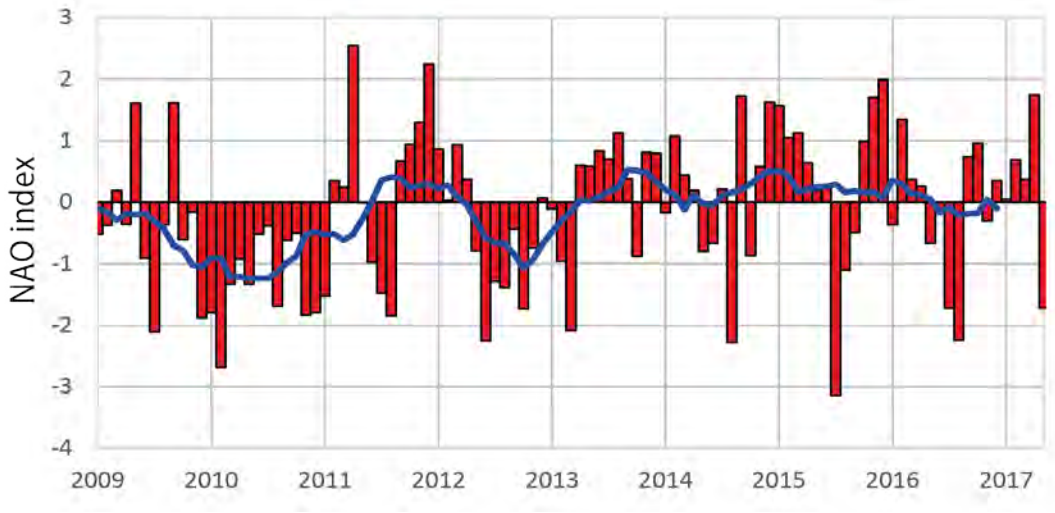

Figure 2: Monthly NAO indices for the period from 2009 to 2017 (climatology based on 1981–2010 period). The dark blue curve shows the 11 months running average. Data retrieved from ftp.cpc.ncep.noaa.gov/wd52dg/data/indices/tele_index.nh.

2.2 Climate variability in future scenarios

Due to the natural variability in the climate described above, the future path of air temperatures over Nunavik and Nunatsiavut will not follow a smooth upward trajectory as shown in multi-model averages (e.g., Figure 3.1 in AMAP, 2017c), and temporary local cooling trends, with durations of up to 25 years or more, can be expected with significant probabilities (Grenier et al., 2015). For the region, particularly for the Nunatsiavut, a key question is whether future warming has the potential to modify climate variability linked to the Atlantic meridional overturning circulation (AMOC). Observations suggest a weakening of the AMOC by ~15 % over the past 150 years in response to freshening of water in the North Atlantic, which is argued as evidence that AMOC is responding to climate change rather than driving it (Thornalley et al., 2018). Additional evidence for this argument is provided by recent high resolution climate model simulations that show a weakened AMOC as a plausible feature of the future climate (Caeser et al., 2018). The consequences of a weakening of the AMOC are large-scale relative cooling of the subpolar gyre region over the northwest Atlantic (by ~1K in the Caeser et al. (2018) CO_2-doubling experiment) due to reduced heat transport that is most pronounced during winter and spring. Another potential consequence of continued freshening of the North Atlantic is sudden rapid cooling events linked to collapse or disruption of the AMOC (Sgubin et al., 2017). The climatic implications of any sudden cooling event over the northwest Atlantic on the climate of Nunavik and Nunatsiavut is difficult to specify, but would more likely be felt over the coastal region of Nunatsiavut as a slowdown of the projected warming trend. The consequences of a disruption of the AMOC are more critical for Europe where heat transport from the Gulf Stream has a major impact on winter climate. Two of the three global climate models used to drive the RCM scenarios presented in this update (CanESM2 and MPI-ESM) are indicated by Sgubin et al. (2017) as not containing any evidence of abrupt cooling events. The scenarios presented here may therefore be somewhat conservative, but this is prudent for long-term planning purposes. The results of the Sgubin et al. (2017) analysis did not address to what extent rapid cooling events are part of the natural climate variability of the region. This is considered a priority question for future study and would require analysis of large ensembles from models capable of simulating the AMOC and its observed sensitivity to freshening.

Another issue and rapidly evolving research topic is the potential role of amplified Arctic warming and declining Arctic snow and ice cover in modifying the strength of the polar vortex and mid-latitudinal circulation (e.g., Francis et al., 2017; Overland et al., 2016; Barnes and Screen, 2015; Cohen et al., 2014; Francis and Vavrus, 2012). The issue of importance for the region, particularly Nunatsiavut, is whether the weakening of the polar vortex will preferentially push

the NAO-AO into a negative phase associated with warmer and wetter atmospheric circulation over the region. There is evidence that the polar vortex has weakened in recent years, but the link between amplified Arctic warming and NAO-AO is not robust in model simulations (Francis et al., 2017), and exhibits high sensitivity to the location of sea ice loss (Screen et al., 2018; Pedersen et al., 2016). In an earlier modeling study, Fyfe et al. (1999) found that warming had no discernible influence on AO phase. However, it is still unclear if current-generation climate models adequately capture the atmospheric response to sea-ice change, and further research and improvements in model horizontal and vertical resolution are needed to obtain a more realistic representation of the processes and feedbacks involved in Arctic and sub-Arctic regional climate dynamics (Screen et al., 2018; Overland et al., 2016).

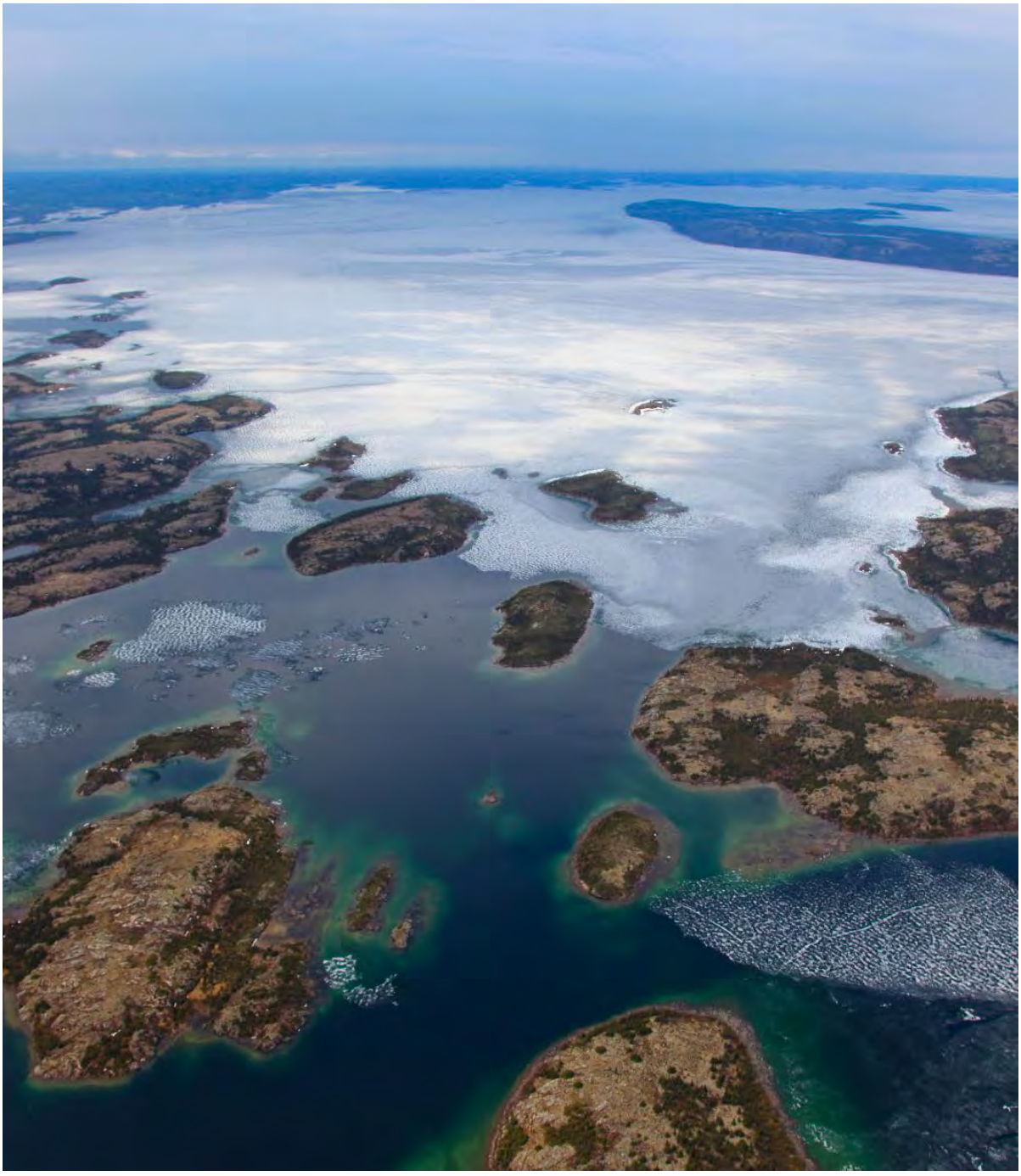

3. Observed and projected changes in regional climate

This section presents a summary of observed and projected changes in key climate indicator series related to air temperature, precipitation, snow cover, wind, waves, sea ice, and the period for safe travel over sea ice.

3.1 Air temperature and related indices

3.1.1 Observed air temperature variability and trends

Air temperature is a key driver of climate and environment in Nunavik and Nunatsiavut through its wide-ranging impacts on snow and ice cover, ground thermal regime, vegetation and many other systems. The spatial pattern of mean annual air temperature for the reference period of 1980 to 2004 (Figure 3) shows a clear north-south gradient in Labrador and northern Québec with the coldest temperatures over the Ungava Peninsula and Torngat Mountains, and the warmest over southeastern coastal regions of Labrador. There is also a strong coastal gradient in mean annual temperature and annual temperature range along the coast of Nunatsiavut. Evidence from dendroclimatological data in Labrador (52–55°) positions the transition from maritime to continental climate approximately 330 km inland from the coast (Nishimura and Laroque, 2011) in agreement with meteorological observations (Way et al., 2017).

The observed mean annual air temperature trends included in this update are based on the Way et al. (2017) 1-km gridded monthly surface air temperature dataset covering eastern Canada for the period 1948–2016. The advantages of the Way et al. (2017) dataset are that it incorporates more surface observations than other surface climate datasets such as CRU, and is provided at a higher spatial resolution. The CANGRD dataset (Milewska et al., 2005) based on interpolated (~50 km grid) climate station data adjusted for systematic errors (Vincent et al., 2012) was used for analysis of trends in annual maximum and minimum air temperature. Regionally averaged seasonal air temperature time series for Nunatsiavut and Nunavik show quite similar historical variability as much of the region is influenced by common sources of atmospheric (e.g., North Atlantic Oscillation) and oceanic (e.g., Atlantic Multidecadal Oscillation) variability (Way and Viau, 2014).

Figure 4, updated from Way and Viau (2014), is therefore a good proxy of historical variability in mean annual air temperature for the entire region since 1850. There is clear evidence of long-term warming of ~1.0 °C/100y over the period of record, with the period since ~1970 showing pronounced multi-decadal variability related to a range of climate forcing mechanisms including salinity anomalies, volcanic activity, and anomalies in atmospheric and oceanic circulation. For example, the large positive/negative regional mean annual air temperature values in 2010/2015 are linked to anomalies in NAO and NW Atlantic sea surface temperatures that act to reinforce regional warming/cooling. Both natural and anthropogenic forcing are significant factors in explaining the observed warming over the past two decades (Finnis and Bell, 2015; Way and Viau, 2014).

Significant warming of the mean annual air temperature over the last 30 years occurred in most communities in the region at a rate of 0.5 to 0.9 °C/decade. The recent 30-year period (1987–2016) is characterized by stronger temperature increases in winter (January-March) with regionally averaged winter trends exceeding 1.5 °C/decade in both Nunavik and Nunatsiavut (Figure 5). The monthly air temperature warming trend in the recent 1987–2016 period is more pronounced than the longer term period 1948–2016. This recent period is also characterized by widespread significant summer warming ~0.5 °C/decade over the region.

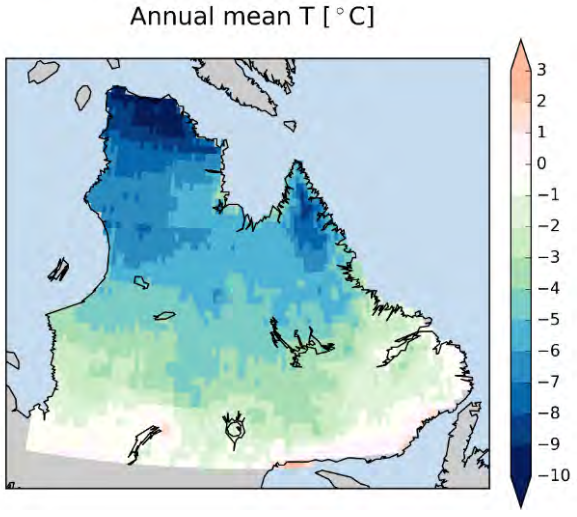

Figure 3: Climate reference map for the mean annual air temperature for the period 1980–2004 obtained from the AgMERRA dataset (Ruane et al., 2015).

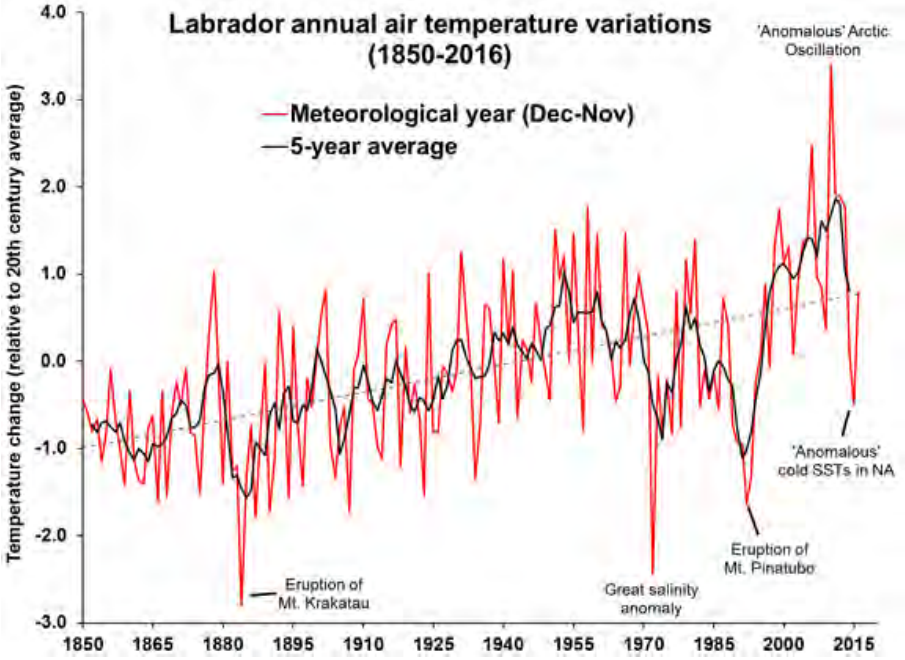

Figure 4: Historical variability in Labrador air temperature anomalies updated from Way and Viau (2014).

Box 1. Scenario construction methodology:

The scenario construction method follows Mailhot and Chaumont (2017) and is based on the "delta method" which computes the difference (Δ) between a future climate mean state (*Fut*), and a current climate or reference state (*Ref*) which can be shown in equation (1) as:

$$\Delta_x = \overline{X}_{Fut} - \overline{X}_{Ref} \quad (1),$$

where $\overline{X}_{Fut}$ is the mean climate index value over the future period and $\overline{X}_{Ref}$ is the corresponding value for the reference period.

A 25-year (1980–2004) period was used as the reference with projected changes computed from the CORDEX regional climate model ensemble for two future periods – mid-century 2040–2064 (H50) and end-of-century 2076–2100 (H85) – and two emission scenarios, RCP 4.5 and RCP 8.5. A 7- or 11-member ensemble of regional climate model (RCM) simulations was used from 5 or 8 RCMs depending on the emission scenario (see summary of the simulations used in Tables A-4 and A-5 in Appendix A). An evaluation of the RCM simulations against the full CMIP5 ensemble over northern Québec showed the RCM simulations adequately represent the spread in the CMIP5 model projected changes in temperature and precipitation over the region (Mailhot and Chaumont, 2017). The bias distribution between surface observations and climate models, presented in the form of a violin plots (Diaconescu et al., 2017; Hintze and Nelson, 1998), was used as a guideline on how well the climate models simulate the observed reference climate. The consistency in the sign of projected change over the model ensemble was assessed by flagging grid points where more than 10 % of models had changes of opposite sign to the median.

The indices presented throughout the update are based on previous discussions with scenario user groups from the 1st iteration of the report (Allard and Lemay, 2012) and extended on the basis of a concurrent project involving the Ministère des Forêts, de la Faune et des Parcs (MFFP), Ouranos and Institut national de la recherche scientifique (INRS). As outlined in Diaconescu et al. (2017), the extended set of climate indices selected for analysis are based on recommendations made by the Expert Team on Climate Change Detection and Indices (ETCCDI; Klein Tank et al., 2009). The indices are summarized in Tables A1 to A4 in the Appendix A.

The reason why statistical significance (emergence of the "signal" from the "noise") covers a smaller fraction of Nunavik and Nunatsiavut for winter (relative to summer) despite the larger trends is that the year-to-year standard deviation is larger. Thawing season start and end dates for the most recent 30-year period show systematically earlier start (2–3 days/decade) and latter end (3–5 days/decade) dates at the regional scale (Figure 6). Warmer summer conditions have also been linked to rapid shrub growth across Nunavik and Nunatsiavut (Ju and Masek, 2016; Fraser et al., 2011) with corresponding thermal effects on permafrost (Way and Lewkowicz, 2016) and wildlife (Fauchald et al., 2017; Whitaker, 2017). Warmer summers are also implicated in the rapid shrinkage and thinning of small mountain glaciers in northern Nunatsiavut (Barrand et al., 2017; Way et al., 2015).

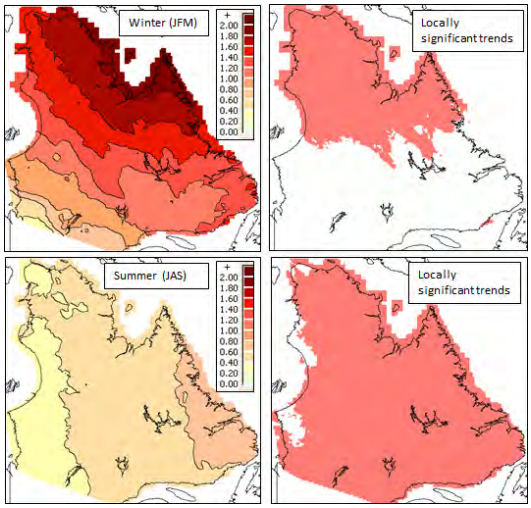

Figure 5: Observed 1987–2016 trend (°C/decade) in winter (top) and summer (bottom) mean monthly air temperature from the Way et al. (2017) dataset. Grid points with locally significant (0.05 level) trends are shown in red in the panels.

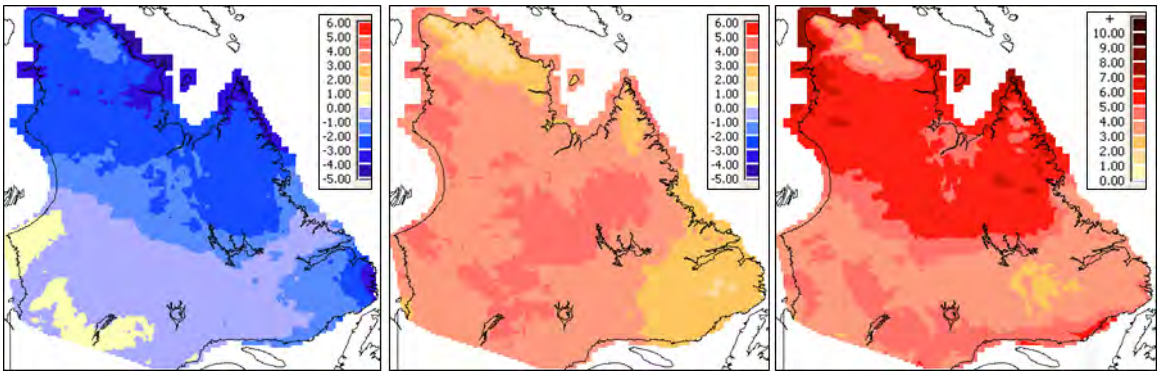

Figure 6: Observed 1987–2016 trends in the onset date (left), end date (middle) and duration (right) of the period of the year with above-freezing temperature from the Way et al. (2017) monthly temperature dataset. Zero-degree Celsius crossing dates are estimated from spline fits to the monthly temperatures. Trend units are days/decade for all three plots. The negative trends in the onset date reflect earlier spring thaw, while the positive end date trends reflect later freeze-up.

3.1.2 Projected change in air temperature

Air temperature is projected to warm significantly over Nunavik and Nunatsiavut during the 21st century (Table 1) with the largest warming (+6.7 °C for RCP 8.5) occurring after ~2050 (Figure 7b). On the annual basis, projected changes are largest in the winter period (Figure 7c) with changes up to +3–13 °C. The spatial pattern of projected change shows the largest warming occurring over northern portions of the region (Figure 8), and is consistent with results presented in the previous IRIS-4 assessment (Allard and Lemay, 2012) and in AMAP (2017c).

The projected warming is expected to cause an increase in growing degree-days (cumulative degree days >5 °C; Figure 9), a longer summer season length (Figure 10), and an increase in the frequency of warm days (percentage of days when daily maximum temperature is greater than the 90th percentile of daily maximum temperature). Increases are also expected in the number of very warm days (Figure 11) and very warm nights. The regional median of the projected changes in annual warmest temperature shows a clear positive sign of change for RCP 8.5 respectively for periods H50 and H85 (~2.3 and 4.3 °C; Figure 11); however, the change is less rapid than the median of

the mean annual temperature (Figure 7b). Cold extreme temperature changes appear to be driving most of the change on an annual basis with positive signs of changes projected for the end of the century in both the annual coldest temperature (RCP 8.5) for periods H50 and H85 (~7 and 15 °C) and the extreme cold nights (6 and 13 °C).

Overall, projected warming is expected to have wide-ranging impacts. For example, built infrastructure (housing roads and other linear infrastructure) is particularly sensitive to thawing of the underlying permafrost that is highly sensitive to warming temperature. Significant changes to the region's vegetation have already been observed at many sites in the region, as well as changes to caribou population dynamics that are at least partly related to the warming temperatures (Zamin et al., 2017; Leblond et al., 2016). Changes to the water quality can also be expected as well as impacts on food security, food quality and mental health at the community and household level. Warmer and more frequent warm temperature extremes are likely to place additional stress on natural and human systems but there are some positive impacts associated with warming such as reduced heating costs and related fossil fuel consumption.

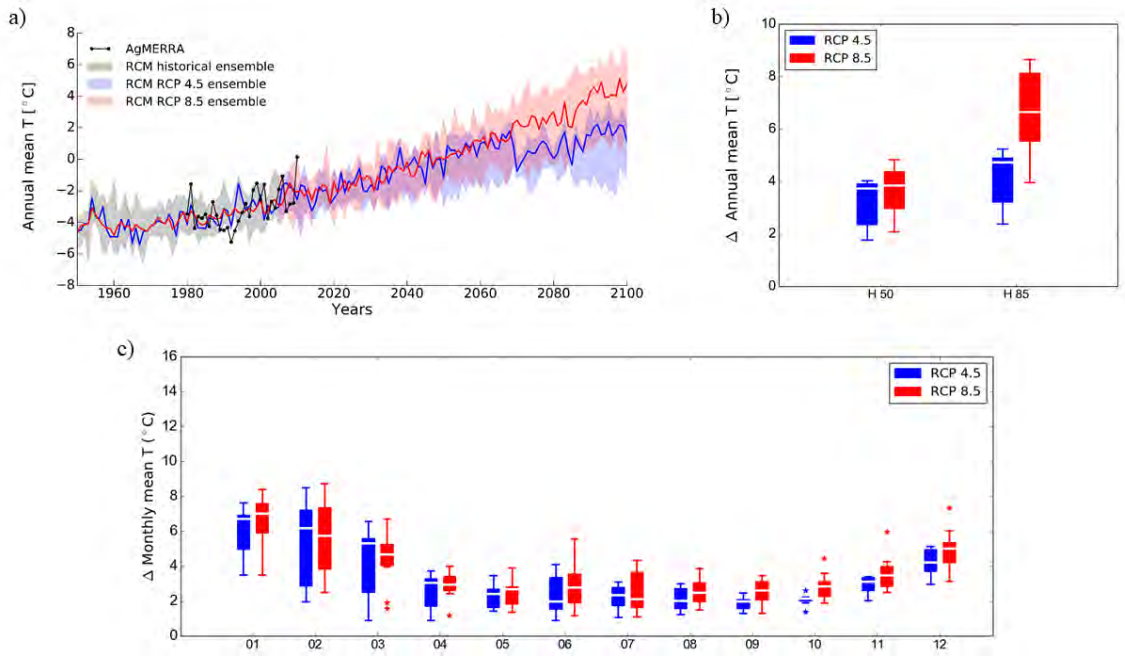

Figure 7: a) Time evolution of mean annual air temperature averaged over Nunatsiavut and Nunavik. The blue zone corresponds to the RCP 4.5 ensemble of 7 RCM simulations from 2006 to 2100, while the central blue line shows the ensemble median. The red zone corresponds to the RCP 8.5 ensemble of 11 RCM simulations from 2006 to 2100 with the median of the simulations represented by the red line. The gray zone corresponds to the historical RCM ensemble of simulations (11 simulations) from 1950 to 2005. Each RCM simulation was corrected to have the same 1980–2004 mean as the reference climate (the black line). b) Box plot of regionally-averaged change in mean annual air temperature for RCPs 4.5 and 8.5 for periods H50 (2040–2064) and H85 (2076–2100). c) Regionally-averaged projected change in mean monthly air temperature for the RCP 4.5 ensemble (blue), the RCP 8.5 ensemble (red) for the H50 period.

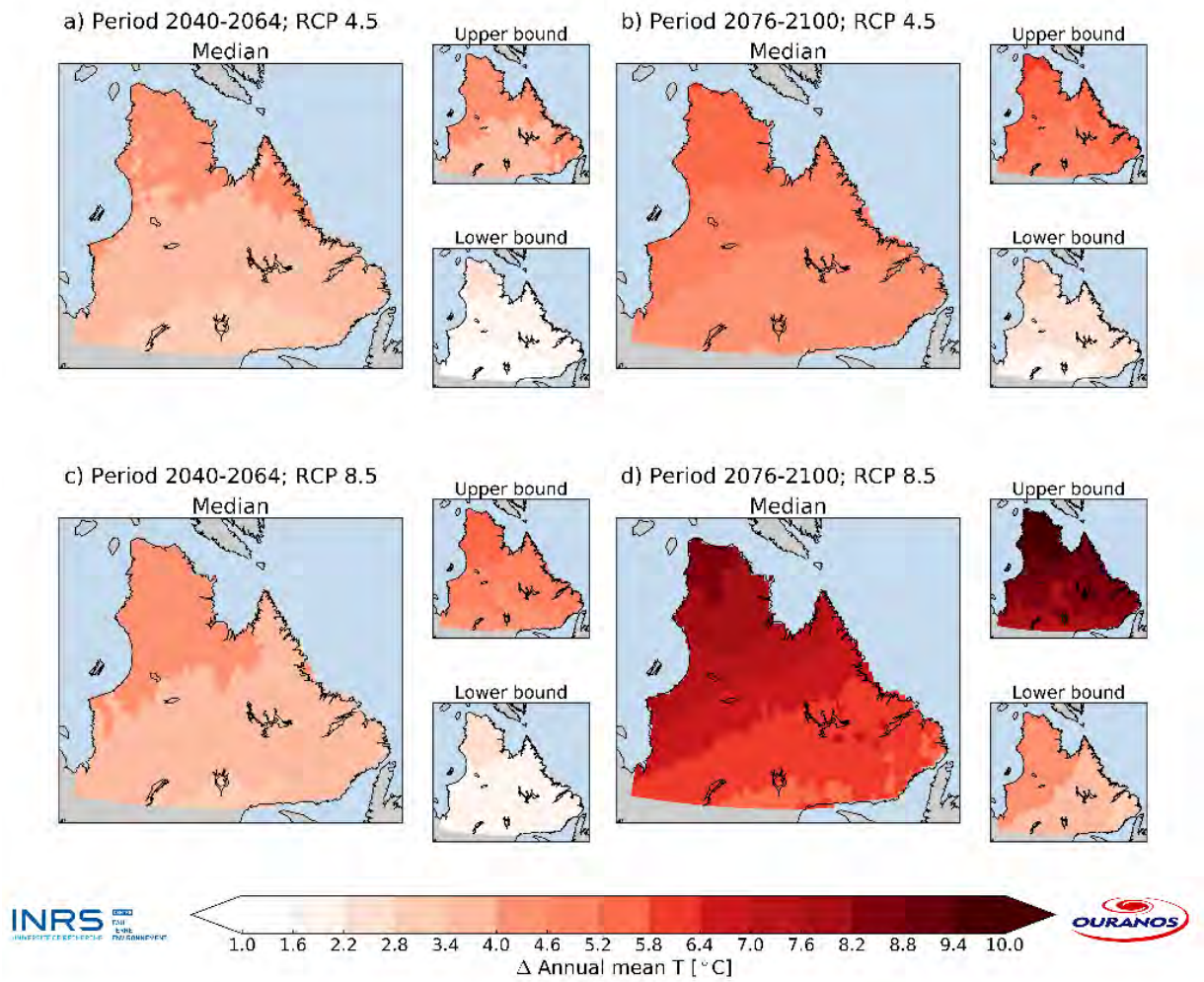

Figure 8: Projected change in mean annual air temperature from an ensemble of RCM simulations for two periods 2040–2064 (H50) and 2076–2100 (H85) and two greenhouse gas emissions scenarios (RCP 4.5 using 7 simulations and RCP 8.5 using 11 simulations). The central map of each panel in (a, b, c and d) shows the median of the simulated differences at each grid-point. The two secondary maps presented next to each central map of each panel (a, b, c and d) give an indication on the dispersion of projected changes in the model ensemble: the “Upper bound” shows the simulation with the largest mean change over the domain, while the “Lower bound” shows the simulation with the smallest mean change over the domain.

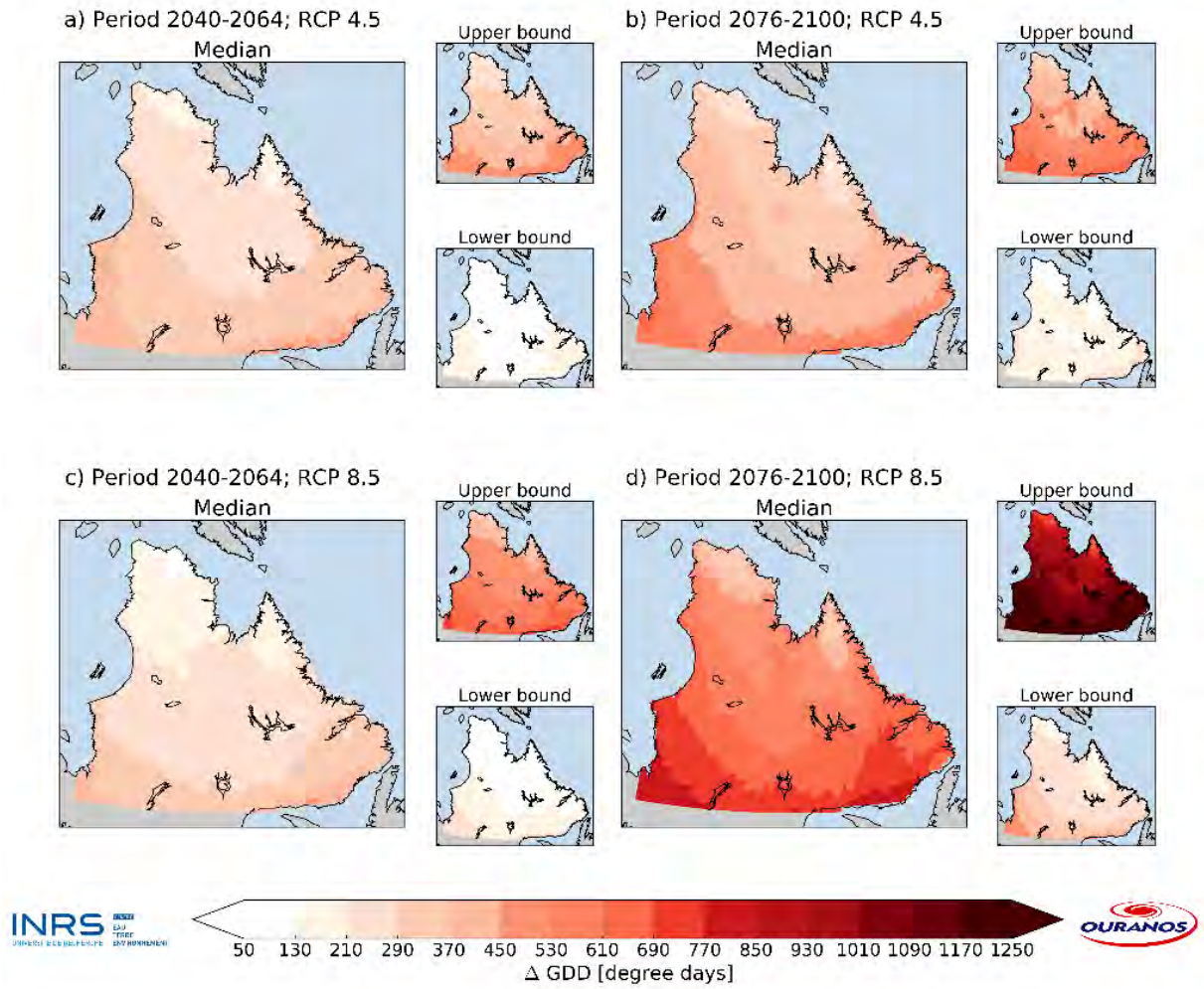

Figure 9: Same as Figure 8 for projected changes in growing degree days.

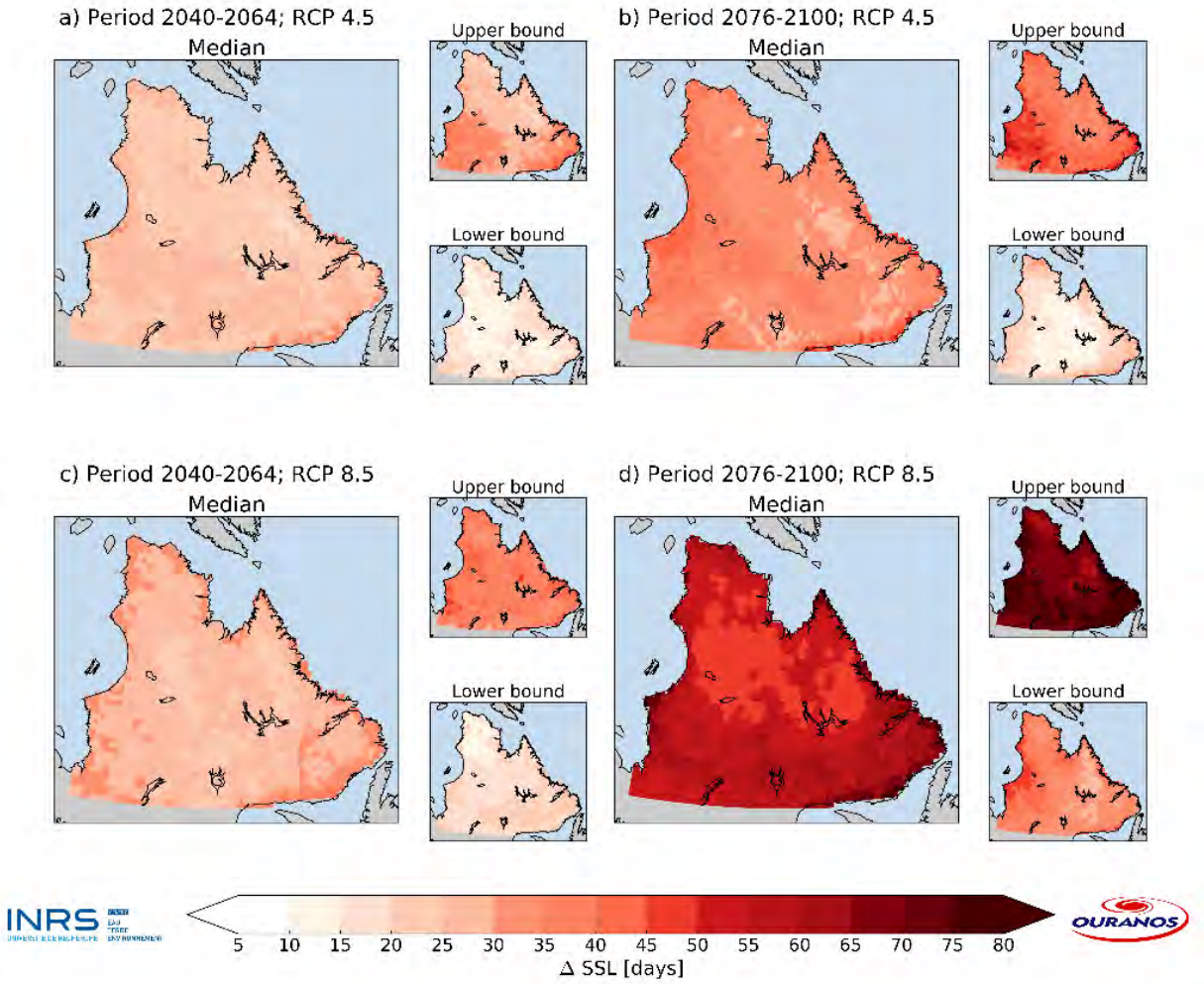

Figure 10: Same as Figure 8 for projected change in summer season duration.

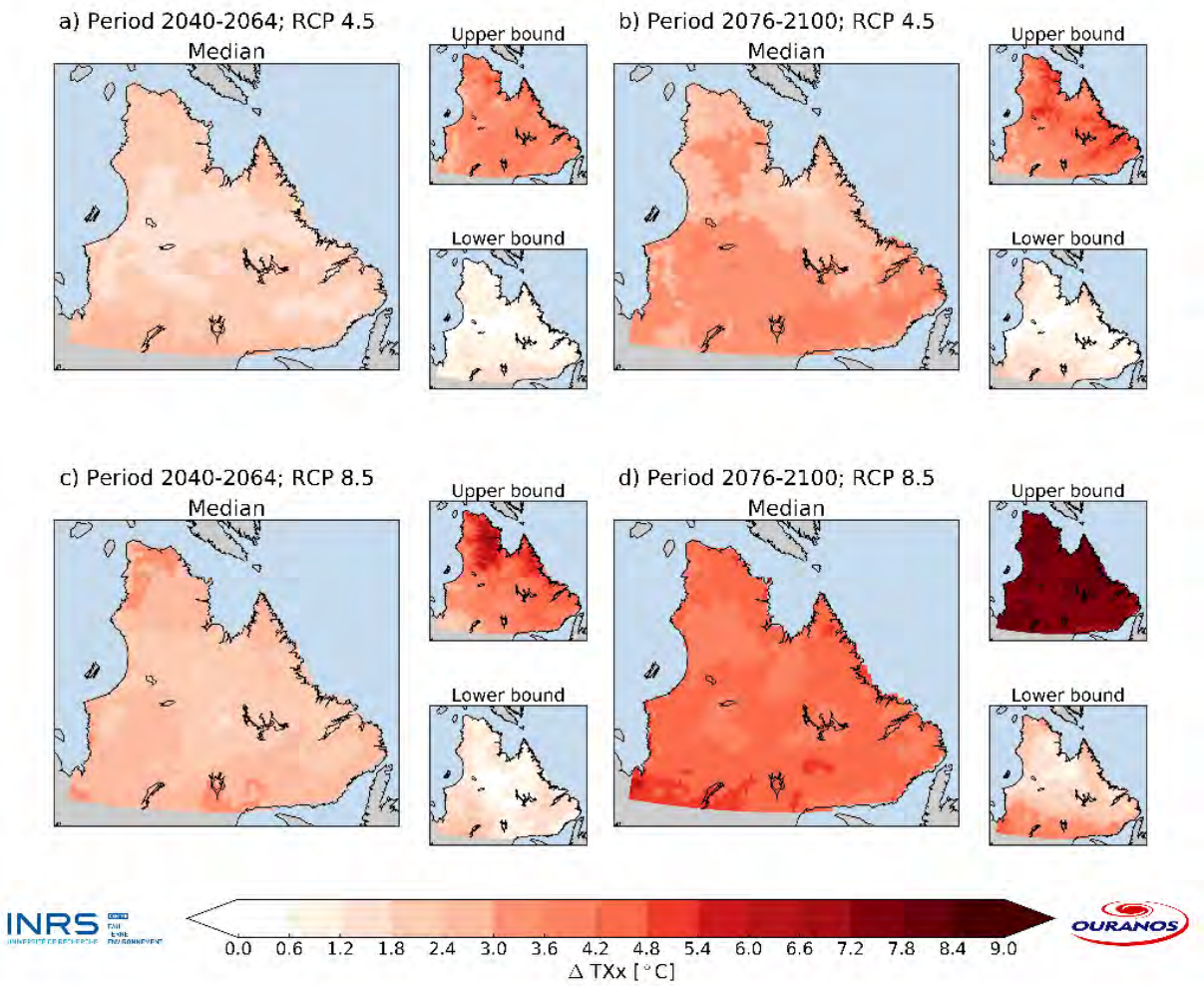

Figure 11: Same as Figure 8 for projected change in the annual maximum value of daily maximum temperature.

Table 1: Summary of the projected climate changes for indices related to air temperature for the H50 period (the first line) and the H85 period (the second line). The range indicated corresponds to RCPs 4.5 (first value) and 8.5 (last value).

Climate indices	Nunavik		Nunatsiavut	
	Projected Change **H50: RCP4.5 to RCP8.5** **H85: RCP4.5 to RCP8.5**	**Comments**	**Projected Change** **H50: RCP4.5 to RCP8.5** **H85: RCP4.5 to RCP8.5**	**Comments**
Annual mean T (°C)	+2.8 to +5.7 +2.8 to +8.7	South to north gradient with largest changes over the northern most part of Nunavik.	+3.4 to +4.5 +3.4 to +7.5	Change patterns similar to the Nunavik region.
Thawing (degree days)	+211 to +713 +255 to +1050	Changes are stronger in the south and over the coastal region of Hudson Bay and southern Ungava Bay.	+211 to +449 +211 to +949	Largest changes over the southern coast.
Nthaw (days)	0 to +3 -3 to +3	No clear evidence of change in winter thaw events as potential increases are offset by a decrease in winter season length.	0 to +3 -3 to 0	No clear evidence of change in winter thaw events as potential increases are offset by a decrease in winter season length.
Freezing (degree days)	-1400 to -800 -2450 to -800	Clear south to north gradient with largest change over higher latitudes and elevations.	-1400 to -800 -2450 to -800	Greatest changes are located over the Torngat Mountains.
Growing (degree days)	+130 to +290 +210 to +849	Largest changes projected over Hudson Bay coastal areas.	+130 to +290 +210 to +669	Large changes in the south and coastal regions of Nunatsiavut.
Summer season length (days)	+20 to +34 +20 to +69	Relatively uniform change over the region with larger changes over coastal regions.	+20 to +34 +25 to +64	Relatively uniform change over the region with larger changes over coastal regions.
Max of daily max air T (°C)	+0.6 to +4.1 +1.8 to 5.9	Uniform change over the entire region.	+0.6 to +4.1 +1.8 to +5.3	Uniform change across the region.

3.2 Precipitation and related indices

3.2.1 Observed precipitation variability and trends

Precipitation is a key driver of environmental change with direct impacts on snow cover, permafrost, vegetation, water availability and quality and wildlife dynamics. The datasets used for analysis include CANGRD (Milewska et al., 2005), individual climate stations in or near the region for trend analysis from the Mekis and Vincent (2011) adjusted precipitation data, and the AgMERRA dataset (Ruane et al., 2015) for defining the regional reference climate for the 1980–2004 period.

Precipitation in the region exhibits a large northwest–southeast gradient with mean total annual precipitation exceeding 1000 mm (2.7 mm/day) over the southern coast of Nunatsiavut to less than 400 mm (1.1 mm/day) over the northwestern tip of the Ungava Peninsula (Figure 12). The average number of days with precipitation greater than 1 mm is between 120 and 180 days/year in the south and center of the region while northern Nunavik receives less than 120 days/year of precipitation. The time series of regionally-averaged total annual precipitation from 10 stations in Nunavik and Nunatsiavut in the adjusted precipitation dataset of Mekis and Vincent (2011) shows important interannual and multi-decadal variability with a significant (95 % confidence level) increase of 2–3 %/decade over 1950 to 2014 (Figure 13).

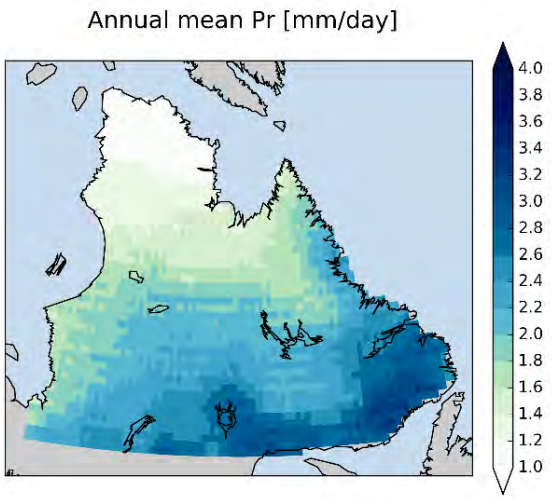

Figure 12: Climate reference map for the annual mean of daily precipitation for the period 1980–2004 obtained from AgMERRA (Ruane et al., 2015).

Analysis of trends in total annual precipitation from multiple datasets over the 1950–2010 period (Rapaic et al., 2015) showed a consensus for significant long-term increases over much of Nunavik, but no trend consensus for Nunatsiavut. Over the more recent 1980–2010 period, Rapaic et al. (2015) showed less evidence of significant trends over the region due to the strong year-to-year variability in total annual precipitation. Analysis of seasonal precipitation trends with the CANGRD dataset over 1980–2014 (Figure 14) shows that summer and fall total precipitation are the primary contributors to changes

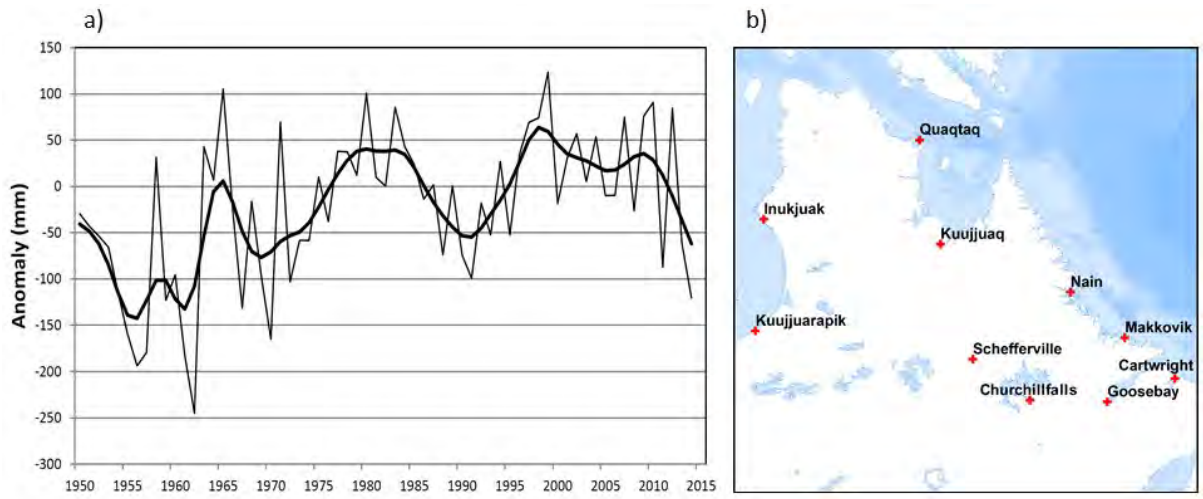

Figure 13: a) Regionally-averaged annual total precipitation anomalies (mm) with respect to a 1971–2000 reference period from 10 stations in Nunavik and Nunatsiavut from the adjusted dataset of Mekis and Vincent (2011). The bold line is the result of applying a 9-term binomial filter. b) Station locations and names.

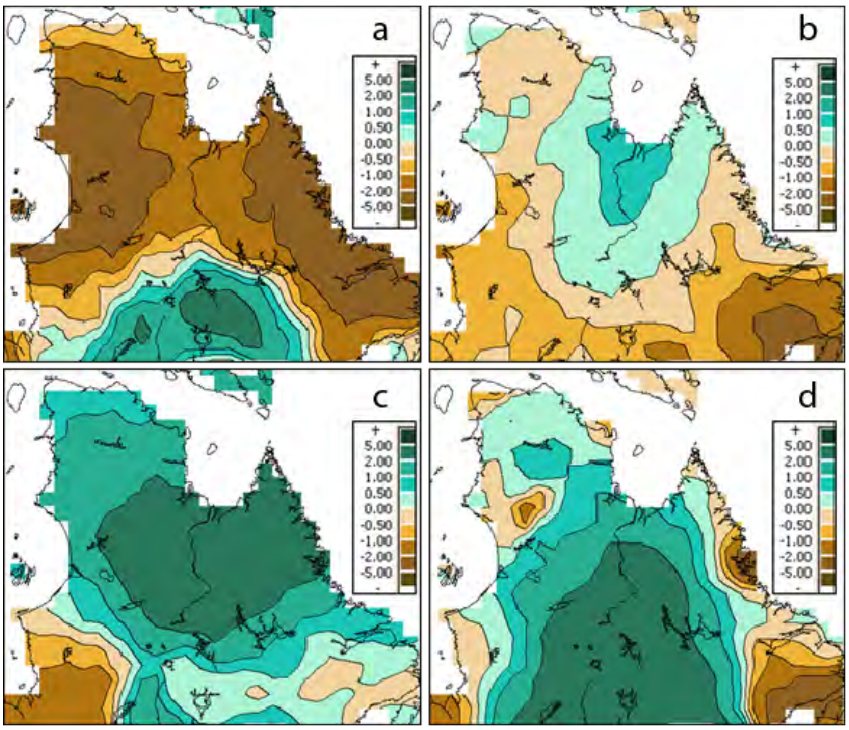

Figure 14: Seasonal total precipitation trends over 1980–2014 (%/decade) for a) winter (DJF); b) spring (MAM); c) summer (JJA); and d) fall (SON) from the CANGRD dataset (Milewska et al., 2005). Percent change is computed with respect to 1981–2010 average precipitation.

in the annual total and account for more than 60 % of the total annual precipitation increase observed at the regional scale. This contrasts with the winter period which is characterized by widespread decreases in precipitation over 1980–2014. The combined influences of decreasing winter precipitation and climate warming are driving significant reductions in annual snowfall over northern Nunavik and Nunatsiavut. Over the period 1980–2014, the solid fraction of annual precipitation in CANGRD, estimated from ERA-interim air temperatures following Brown et al. (2018) is estimated to have decreased significantly from 0.55 to 0.42 in response to warming, with the solid fraction displaying a significant mean annual temperature sensitivity of 0.026/°C which is consistent with the projected decreases in solid fraction provided by the regional climate models in Table 2.

There is no clear evidence of an increasing trend in the intensity or frequency of extreme precipitation over the region in the past decades. This is mainly due to the small number of climate stations located in the region and the length or incompleteness of recorded datasets. Results from Donat et al. (2013) have focused on meridional Québec and showed evidence of spatial variability in the sign of trends for indices of extreme precipitation with few significant increasing trends observed (Ouranos, 2015). Results for the highest 5-days precipitation from Vincent and Mekis (2006) shows opposite signs with increasing trends across Nunavik and decreasing trends in Nunatsiavut (based on two stations in each region for the period from 1950 to 2003). Neither Nunavik nor Nunatsiavut regions are showing significant trends in any of the reported extreme indices which is consistent with the results of Vincent and Mekis (2006) who found strong regional variability in the strength and sign of extreme precipitation trends across Canada.

3.2.2 Projected change in precipitation

Despite the high degree of variability in regional precipitation trends over the past several decades, warming is expected to be a major driver of changes affecting the amount and seasonal distribution of rainfall (Figure 15) and snowfall, and this will have direct impacts on natural and human environment in Nunavik and Nunatsiavut. Projected changes in mean annual daily precipitation (Figure 16 and Table 2) indicate a future wetter climate of 0.24-1.52 mm/day. The spatial pattern in annual daily precipitation is showing relatively homogeneous increases over the region and similar to mean annual air temperature (Figure 7b), the projected increases in precipitation for H85 are strongly dependent on emission scenarios (Figure 15b). The projected absolute change in precipitation is distributed relatively evenly over the year for H50 (Figure 15c). The monthly distribution of precipitation is similar for period H85 though changes are larger (figure not shown). The largest projected changes in annual precipitation are located over the Torngat Mountains with increases of ~1.5 mm/day (Table 2) associated with H85 and RCP 8.5. The frequency of days with rainfall >1 mm is also projected to increase with the largest changes of >30 days over the interior of the eastern coast of Ungava Bay, the Torngat Mountains and the Ungava Peninsula (Figure 17). Projections of 20-year return period extreme precipitation events are estimated to increase to correspond to 7 to 10-year return period events for H50 (Ouranos, 2015). Projected changes in solid precipitation are a response to offsetting influences of warming (reduced duration of the period with freezing temperatures) and increasing precipitation (Krasting et al., 2013), and show a contrasting seasonal response with increases in winter (December-January-February) and decreases in the spring and fall. The largest solid precipitation decreases are projected to occur in October-November. There is no consensus among the ensemble of models on the magnitude of the decrease in solid precipitation for H50 but by H85 most of the region is projected to undergo a decrease in solid precipitation of about -0.15 mm/day (RCP 8.5). The solid fraction of precipitation is also projected to decrease up to -0.19 for RCP 8.5 and period H85 across the Nunatsiavut and Ungava Bay regions (Figure 18). Mean annual solid precipitation shows a clear decrease mostly driven by the stronger changes projected during transition periods (Figure 15c) with especially large changes in the fall transition. This shows the influence of warming air temperature impacts as the summer season is extending to mid-October by H50 and to the end of October by H85. Midwinter solid precipitation shows mostly increases consistent with continued below zero Celsius winter air temperatures and increasing annual precipitation (Figure 15a and b).

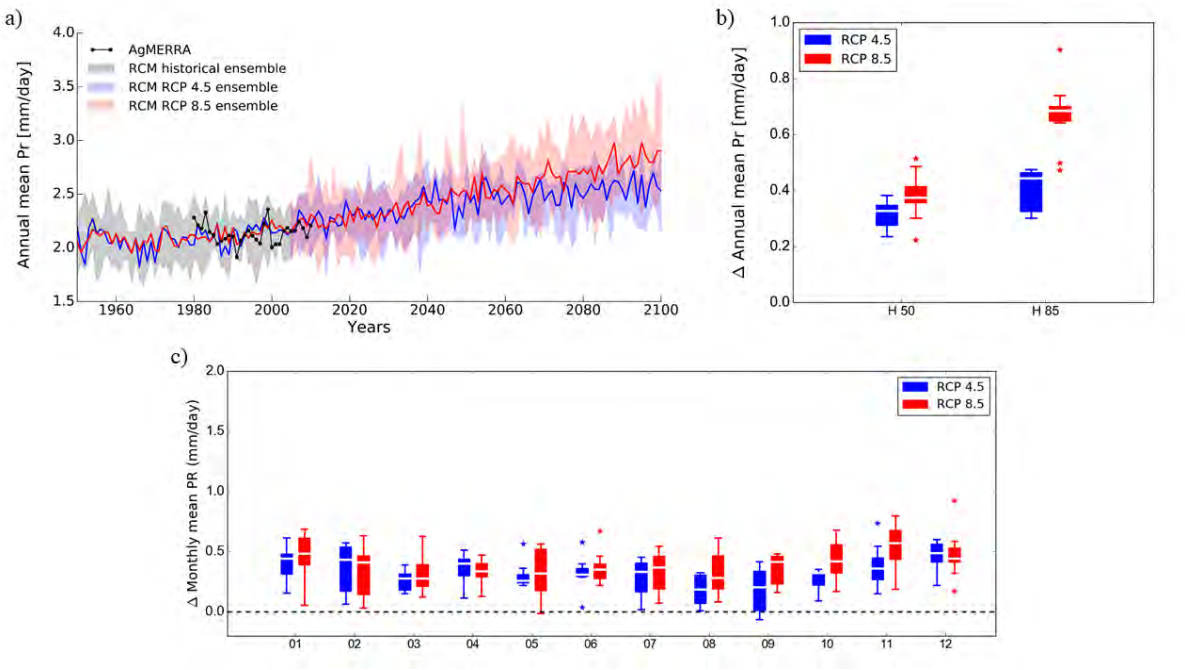

Figure 15: Same as Figure 7 for a) and b) annual mean precipitation (mm/day) and (c) monthly mean precipitation.

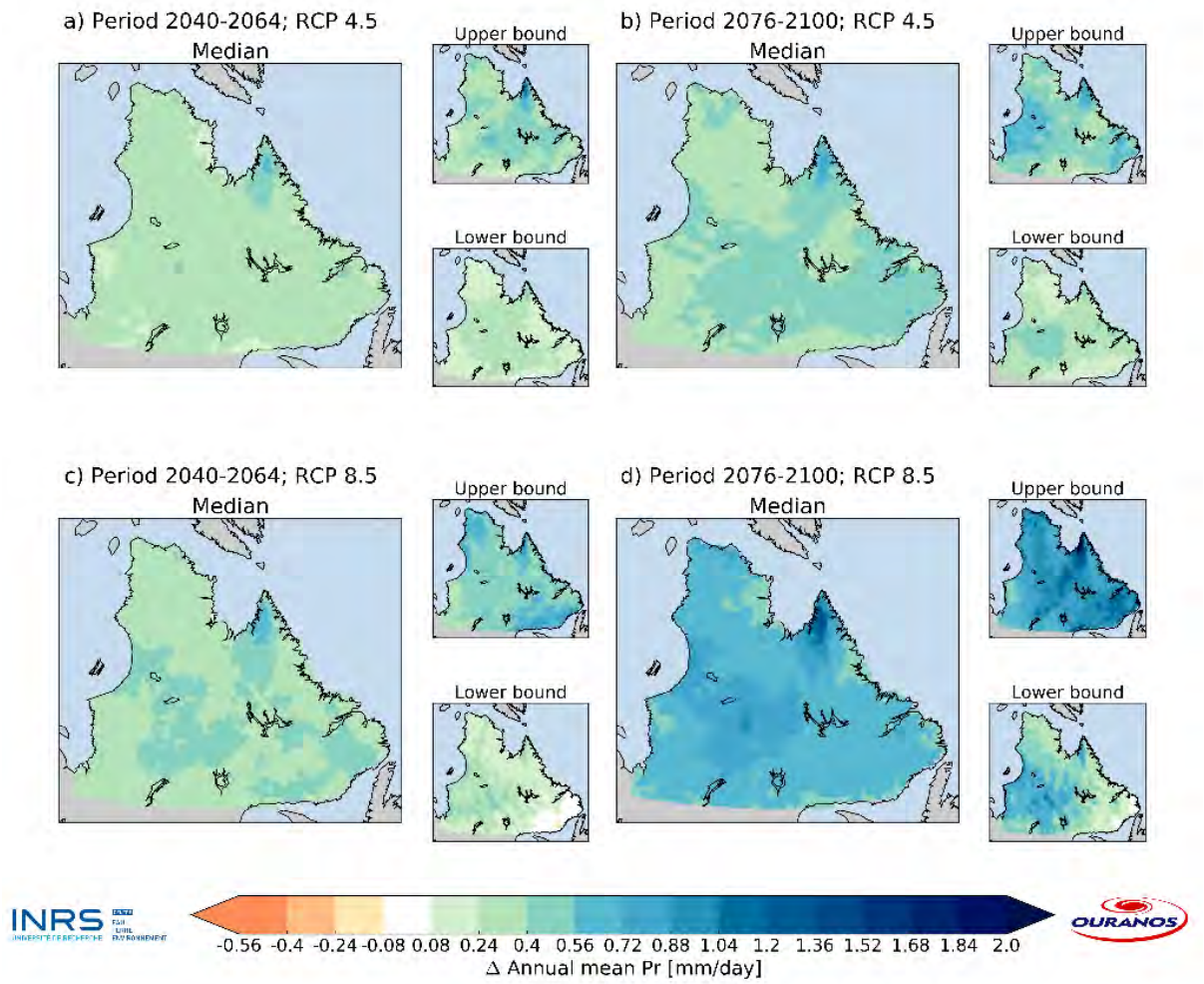

Figure 16: Same as Figure 8 for projected change in annual mean precipitation (mm/day).

In regard to extreme precipitation, the projected change in annual maximum daily precipitation shows increases between about 5 and 10 mm/day respectively for H50 and H85 periods (RCP 8.5). The changes projected for various extreme precipitation indices are systematically stronger than the changes projected for annual mean precipitation, which is a characteristic consistent with reported results from the IPCC report (2013).

Some of the expected landscape impacts of a wetter climate include increases in surface runoff with correspondingly more water and related erosion features, as well as greater potential for active layer detachments in permafrost environments. Likewise, an increase in extreme precipitation events may enhance flood susceptibility in areas where communities are vulnerable as well as increases in water accumulation that may impact some northern infrastructure such as road embankments and airstrips (AMAP, 2017c).

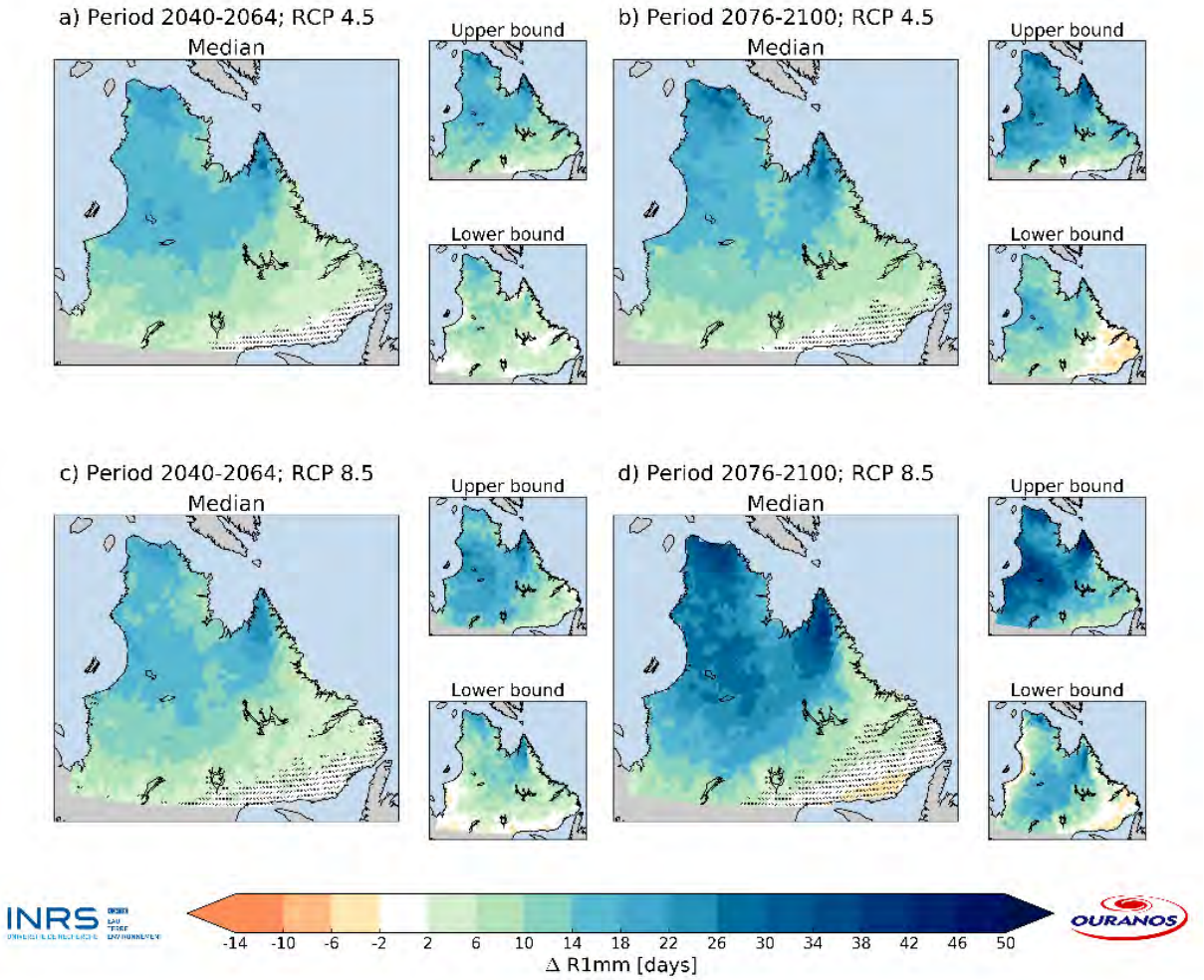

Figure 17: Same as Figure 16 for projected change in the annual number of days with daily precipitation ≥ 1 mm.

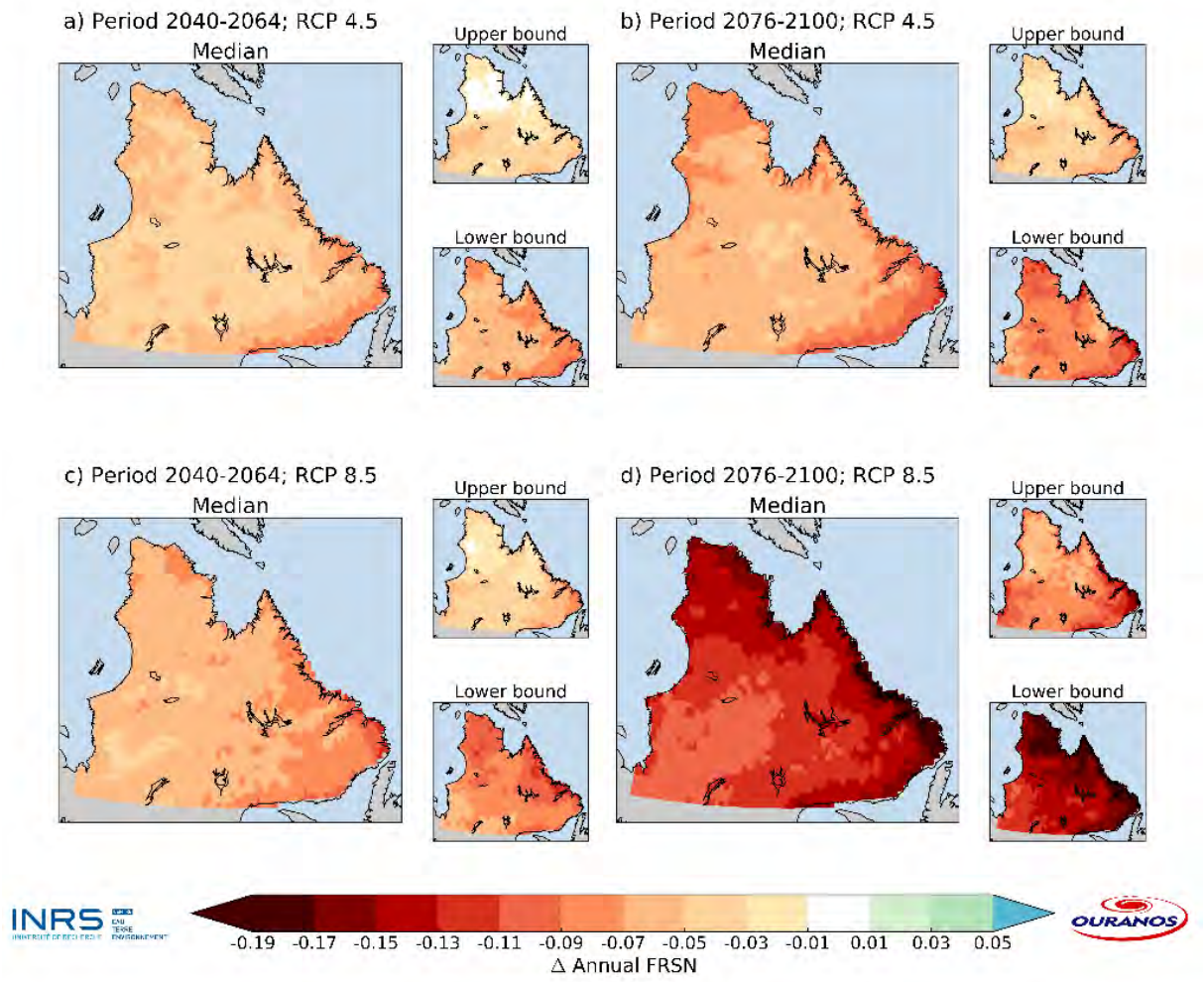

Figure 18: Same as Figure 16 for projected change in the annual fraction of solid precipitation.

Table 2: Summary of the projected climate changes for indices related to precipitation for the H50 period (the first line) and the H85 period (the second line). The lower bond of the interval of values presented in the table corresponds to RCPs 4.5 (first value) and 8.5 (last value).

Climate indices	Nunavik		Nunatsiavut	
	Projected Change **H50: RCP4.5 to RCP8.5** **H85: RCP4.5 to RCP8.5**	**Comments**	**Projected Change** **H50: RCP4.5 to RCP8.5** **H85: RCP4.5 to RCP8.5**	**Comments**
Annual mean daily precip. (mm/days)	+0.24 to +0.89 +0.24 to +1.52	No spatial pattern. Largest increases projected over east Ungava Bay.	+0.08 to +0.72 +0.24 to +1.52	No spatial pattern.
Number of days with precip. ≥ 1 mm/day (days)	+6 to +30 +6 to +42	South to north increasing pattern with largest changes over Ungava Peninsula.	+2 to +26 +2 to +42	Strong coastal (east-west) gradient with largest changes over the Torngat Mountains.
Number of winter rainfall (days)	0 to +2 0 to +2	No clear evidence of change as potential increases are offset by a decrease in winter season length.	0 to +3 0 to -4	No clear evidence of change as potential increases are offset by a decrease in winter season length.
Annual fraction of solid precipitation	-0.11 to -0.05 ≤-0.19 to -0.05	Largest changes show decrease over Hudson Strait coast and Ungava Bay.	-0.11 to -0.05 ≤-0.19 to -0.05	Largest changes over coast of Nunatsiavut.

3.3 Snow cover related indices

3.3.1 Observed snow cover variability and trends

Snow cover is an important component of northern environments and influences a wide range of systems such as permafrost, surface runoff and water levels during spring discharge, vegetation and animal population dynamics (Bokhorst et al., 2016). Snow cover also has important impacts at the local community level through its influence on access to territory, animal behavior, hunting, fresh water, snow clearing, and snow loads (Callaghan et al., 2011). Snow cover characteristics and variability in space and time depend on many factors including proximity to moisture sources (atmospheric and oceanic circulation), latitude, elevation, and local site factors such as topography and vegetation (AMAP, 2017a). There is very little observed data on the depth and water equivalent of snow over the region, thus much of our knowledge about snow cover must be inferred from satellite data and snow models driven by climate data products. For example, the MERRA-2 reanalysis (Bosilovich et al., 2016) was selected as the reference snow cover climate because it best agrees with surface observations over the region. The largest snow accumulations are inferred over the northern tip of the Québec-Labrador peninsula (Figure 19a) due to the combination of locally higher elevations, colder annual mean air temperature and important moisture input from the winter ice-free Davis Strait and Labrador Sea (Langen et al., 2017). This area also has the longest mean snow cover period in the region (~270 days) along with the northern part of the Ungava Peninsula, east of Deception Bay (Figure 19b). There are only five climate stations within or close to the region with long-term daily snow depth observations which are sufficient for assessing past variability and

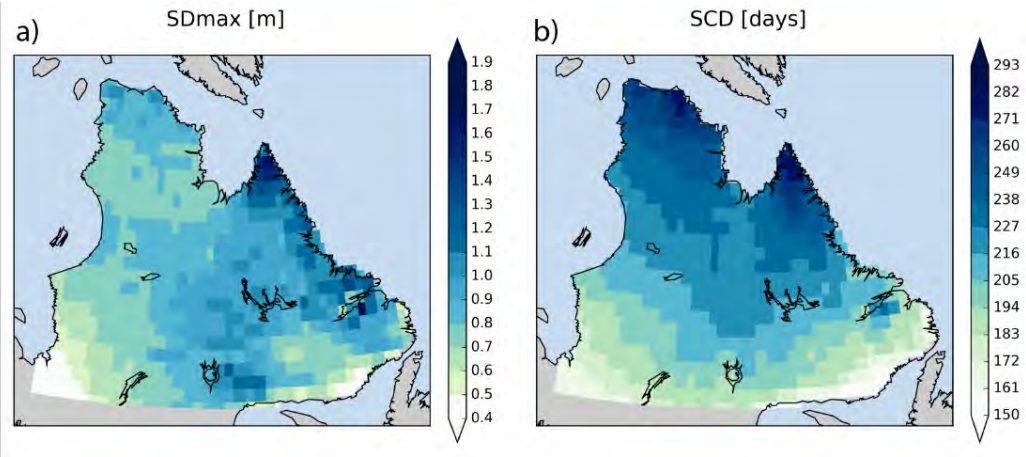

Figure 19: Climate reference maps for a) maximum snow depth and b) snow cover duration for the period 1980–2004 obtained from the MERRA-2 reanalysis.

trends in snow cover (Goose Bay, Cartwright, Nain, Kuujjuarapik and Kuujjuaq). The regionally-averaged anomaly series of first and last dates of snow on the ground from these stations (Figure 20) show evidence of earlier disappearance of snow in the spring (3.9 days/decade) and later onset of snow cover in the fall (3.4 days/decade) that together contribute to a ~40 days shorter snow season currently compared to the late-1950s. Spatially distributed information on snow cover trends over the 1980–2009 period was obtained from the 10-km snow cover reconstruction of Liston and Hiemstra (2011) which confirmed trends toward decreasing snow cover in both halves of the snow season over most of the region (Figure 21) with the exception of northern Ungava and Labrador Peninsulas where snow cover was simulated to start earlier in the season (trend to increased fall period snow cover duration). The stronger declines in spring snow cover duration over the more northern parts of the region is consistent with pan-Arctic trends in spring snow cover which show clear evidence of polar amplification (AMAP, 2017a).

The maximum snow depth anomaly series for the five climate stations in the region (Figure 22) shows evidence of a significant decline over the period since

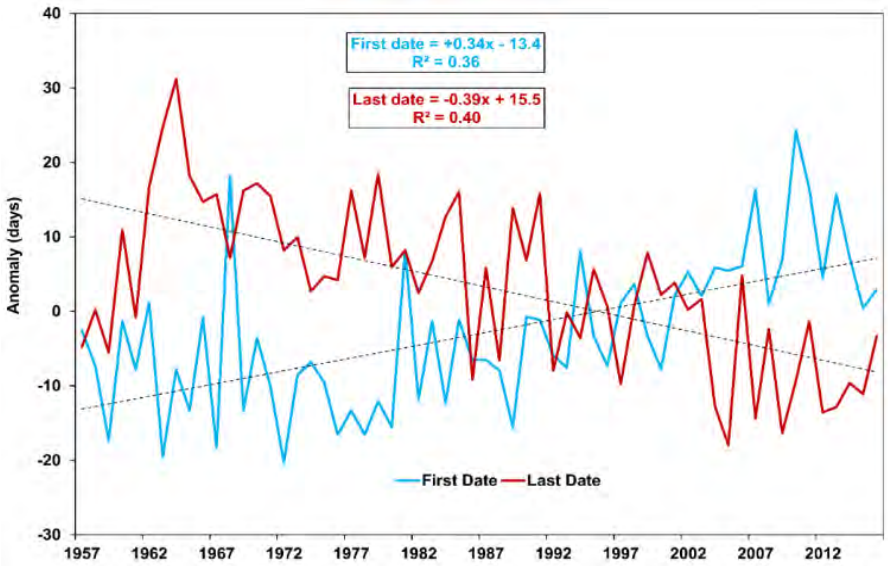

Figure 20: Regionally-averaged time series of the first (blue line) and last dates (red line) of snow on the ground for winters from 1956-57 to 2016-17 for five stations within or close to Nunavik and Nunatsiavut. Anomalies are computed with respect to a 1981–2010 reference period with the trend equation units in days per year. Data source: ECCC digital climate archives.

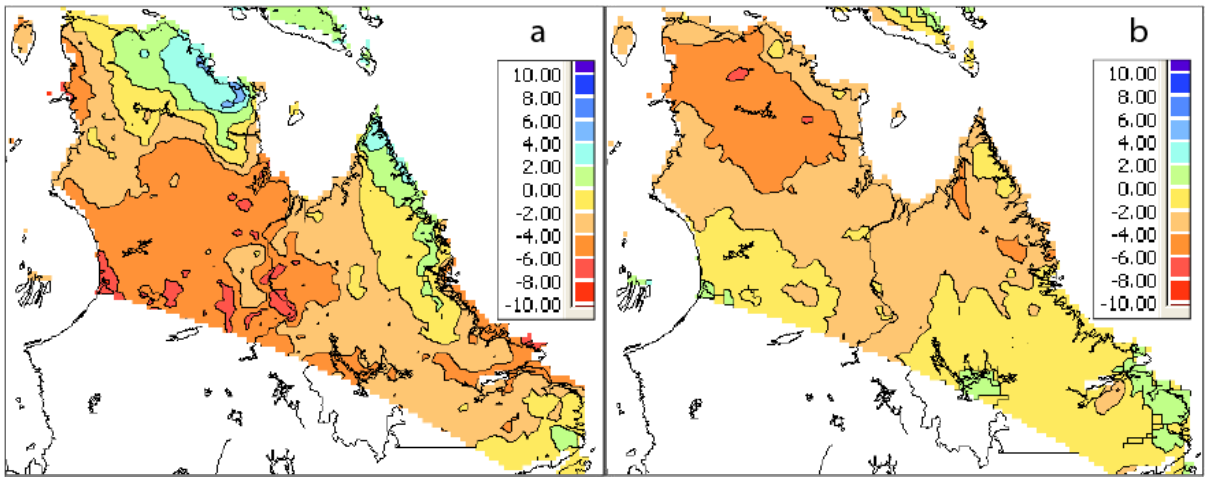

Figure 21: Spatial trend (days/decade) in the duration of snow on the ground in a) the fall (August to January) and b) spring (February to July) halves of the snow cover season from the Liston and Hiemstra (2011) snow cover reconstruction for the period 1980–2009.

1957 of about 25 cm but there are important local exceptions to this trend. For example, maximum snow depth increased at Cartwright over the period by 12.5 cm per decade, while maximum snow depths at Kuujjuarapik also show evidence of increasing over the last 30 years at a similar rate of 10 cm per decade. It is difficult to reach a clear conclusion about snow accumulation trends over Nunavik and Nunatsiavut from this small number of stations and considering the many local-scale factors that can influence snow accumulation. Analysis of trends in maximum annual snow accumulation (not shown) from three different reconstructions (Liston and Hiemstra, 2011), a blend of 5 products by Mudryk and Derksen (2017) and a CRCM5 simulation driven by the ERA-Interim reanalysis revealed quite different trend patterns. However, where the trends were locally significant, they were almost always showing decreasing snow accumulation. The decreasing trend in snow accumulation from the five products is in agreement with the climate stations and local knowledge (Rapinsky et al., 2017; Cuerrier et al., 2015; The Communities of Ivujivik et al., 2005). This finding is consistent with pan-Arctic trends in annual maximum SWE presented in Brown et al. (2017).

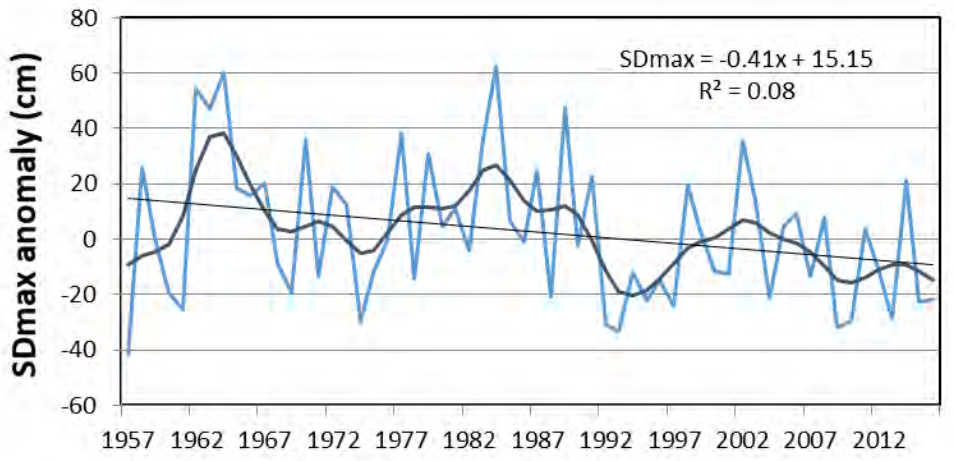

Figure 22: Regionally averaged annual maximum snow depth anomalies from stations over or close to Nunavik and Nunatsiavut for winters from 1956-57 to 2016-17. Anomalies are computed with respect to a 1981–2010 reference period and the smoothed line is the result of applying a 9-term binomial filter. Trend equation units for annual maximum snow depth (cm) change are cm per year. Data source: ECCC digital climate archives.

3.3.2 Observed changes in glaciers

A total of 195 ice masses are located in Nunavik and Nunatsiavut with these features only found in the Torngat Mountains and almost all situated on the Labrador-side of the border. In a 2005 assessment with digital aerial photography, at least 105 of the ice masses showed evidence of active glacier flow (Way et al., 2014). The glaciers of the Torngat Mountains are small in area (0.01-1.25 km^2) and typically found in sheltered mountain cirques between 290 and 1500 m a.s.l. Remote sensing analysis (Figure 23) using geomorphological indices (Way et al., 2015) and 1950s-era aerial photography (Barrand et al., 2017) showed that between the Little Ice Age (est. 1550–1700 AD) and 2005, total glacier area declined by ~53 % with most of the decline occurring between 1950 and 2005 (27 %; Barrand et al., 2017; Way et al., 2015). A further decline in glacier area from 2005 to 2008 of ~9 % was noted by Brown et al. (2012). Cumulatively, total ice mass area in the Torngat Mountains declined from the Little Ice Age maximum of >46 km^2 to <22 km^2 by 2008 (Way et al., 2015; Brown et al., 2012). The rapid decline of glaciers in the Torngat Mountains was also recorded by field and photogrammetry-based surveys compiled between 2005 and 2011 for three of the largest glaciers in the Torngat Mountains (Barrand et al., 2017). These data showed substantial glacier thinning across all three glaciers with average geodetic mass balances between -1.2 m yr^{-1} and -0.5 m yr^{-1} (Barrand et al., 2017). These results highlight the sensitivity of Torngat glaciers to observed changes in regional climate described in sections 3.1.1 and 3.2.1.

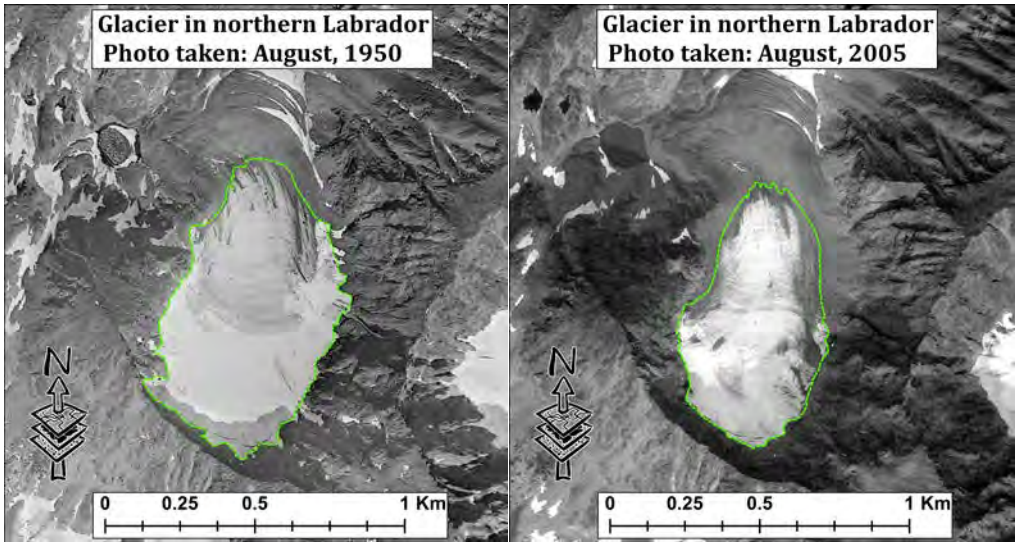

Figure 23: Aerial photographs of a small mountain glacier (59.5 °N, 64.0 °W) in northern Labrador in 1950 (left panel; green outline) and 2005 (right panel; green outline) after Barrand et al. (2017). In 1950, the glacier covered 0.42 km^2 but has since shrunk to 0.3 km^2 in 2005 corresponding to a ~28 % decrease in area over the 55-year period.

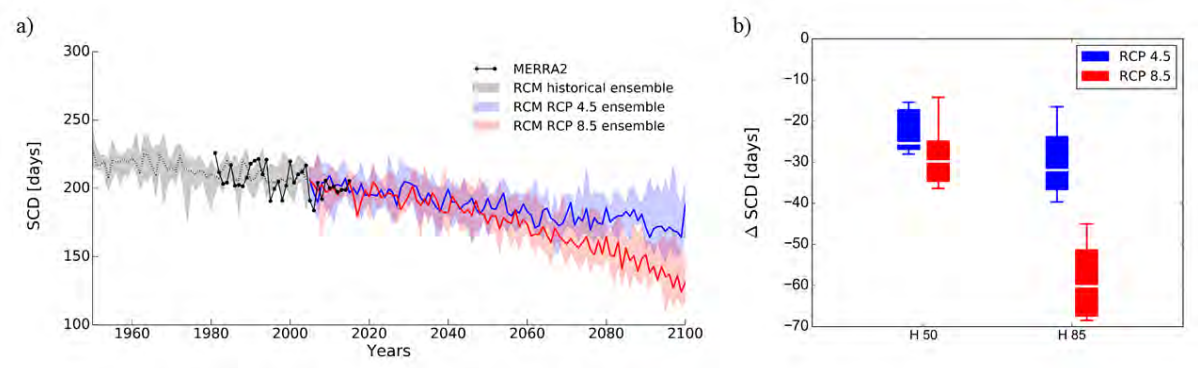

Figure 24: Same as Figure 7 for annual snow cover duration.

3.3.3 Projected change in snow cover

Climate model projections show a clear decrease in snow cover duration by about 30 days for H50 to about 60 days for H85 period under emission scenario RCP 8.5 (Figure 24a and b, and Table 3). This decrease in snow cover duration is mainly driven by warming in the fall (October-November) and spring (May-June) period (Figure 7c) with similar rates of projected change for the start/end dates of snow cover. The maximum annual snow depth (Figure 25) is projected to decrease substantially over coastal regions of Nunatsiavut with smaller decreases over the central region. The observed increasing trends reported from stations in the regions of Cartwright and Kuujjuarapik are not expected to be continued during the next decades considering the projections. Over northern areas of Nunavik, there is no model consensus for the sign of the change and some models project increasing snow accumulation over more northern and/or higher elevated areas of the region.

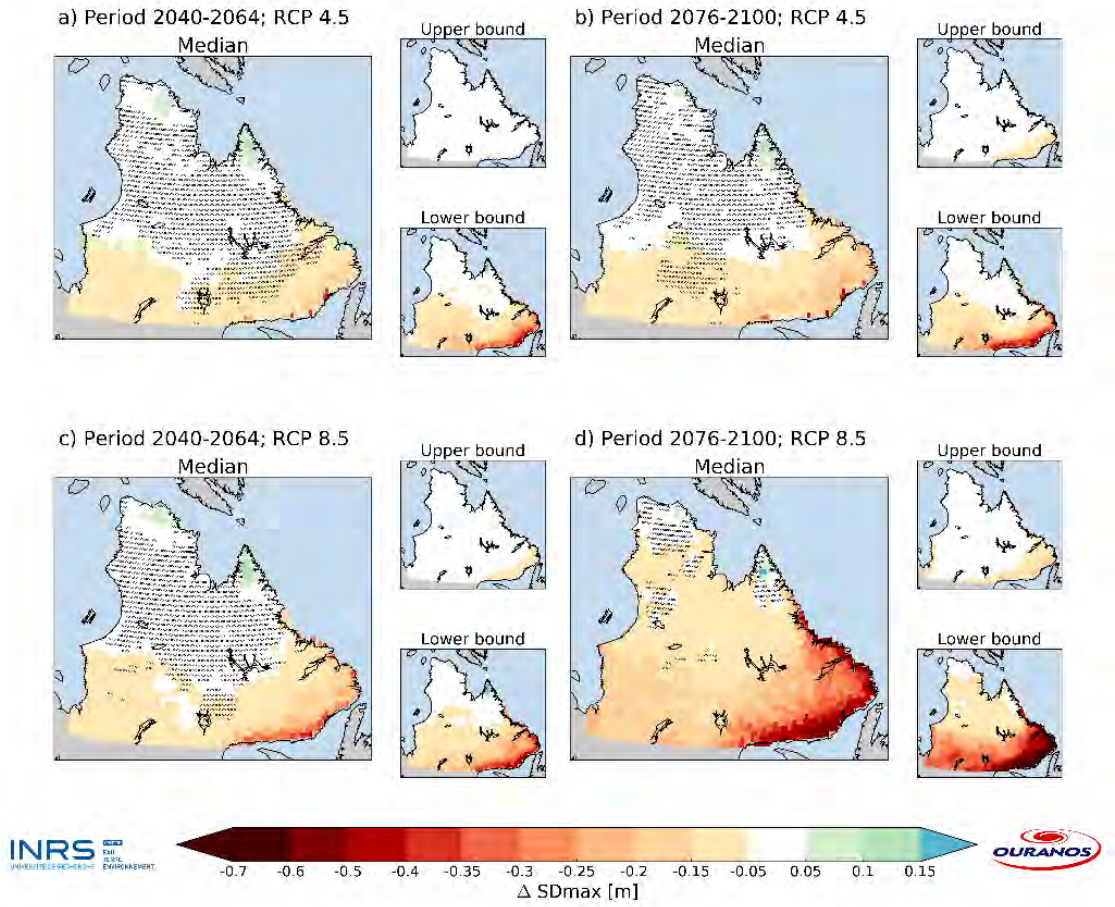

Figure 25: Same as Figure 8 for projected change in annual maximum snow depth. Grid points where more than 10% of models do not agree on the sign of change (positive or negative) are indicated with an "x" i.e., at grid points without an "x", at least 90 % of models project changes with the same sign as the median.

Table 3: Summary of the projected climate changes for indices related to snow cover for the H50 period (the first line) and the H85 period (the second line). The lower bond of the interval of values presented in the table corresponds to RCPs 4.5 (first value) and 8.5 (last value).

Climate indices	Nunavik		Nunatsiavut	
	Projected Change **H50: RCP4.5 to RCP8.5** **H85: RCP4.5 to RCP8.5**	**Comments**	**Projected Change** **H50: RCP4.5 to RCP8.5** **H85: RCP4.5 to RCP8.5**	**Comments**
Snow cover duration (days)	-45 to -15 -75 to -15	Largest duration reduction along coast of Hudson Bay and Ungava Peninsula.	-45 to -15 -75 to -55	Change is relatively homogenous with largest decreases over coastal areas.
Start date of snow cover (days) **+ = later start**	+6 to +22 +10 to +42	Largest change occurs over northern Ungava Peninsula. Northward gradient appearing at H85 RCP 8.5.	+6 to +22 +10 to +38	Changes is slightly more important over the coasts. No spatial pattern.
End date of snow cover (days) **- = earlier end**	-25 to -5 -50 to -5	No spatial pattern. Change is homogenous for H50 but affects coasts and northern interior of Ungava Peninsula at H85.	-25 to -5 -50 to -5	No spatial pattern. Change is homogenous for H50 but affects coastal regions more at H85.
Max snow depth (m)	-0.15 to +0.15 -0.3 to +0.15	Ungava and Labrador Peninsula show local increases. No agreement between models over large areas of Nunavik except for H85 and RCP 8.5 where reductions in max snow depth become more evident.	-0.3 to +0.15 -0.5 to +0.15	No agreement over large areas of Nunatsiavut. Largest regional decreases over coastal areas for H85.

3.3.4 Projected change in glaciers

No detailed studies have been carried out of projected changes in the glaciers in the Torngat Mountains but simulations of the glacier response to warming further north in the Canadian Arctic Archipelago by Lenaerts et al. (2013) suggest mass loss will continue into the future, as enhanced meltwater runoff is not sufficiently compensated by increased snowfall. Simulated glacier volume loss for the Arctic Canada South region (includes northern Labrador and Baffin Island) by Radić et al. (2014) show approximately linear glacier volume losses in response to future warming, with an estimated sensitivity of ~20 % volume loss per °C of mean annual air temperature warming. The observed summer (June-July-August) temperature sensitivity of the Torngat Mountain glacier area from the available survey data is ~ -20 %/°C although multidecadal variability in winter precipitation could moderate this relation (Barrand et al., 2017). The projected annual and summer warming over the region is ~2–4 °C by 2050 under both RCP 4.5 and 8.5 scenarios which suggests that the recently observed declines in glacier ice volume and area are very likely to continue. However, there are major uncertainties in projected changes in maximum annual snow accumulation over the region (Figure 24), and the sheltered topographic position of glaciers in the Torngat Mountains may alter their temperature sensitivity as they retreat deeper into cirque backwalls. Nonetheless, glacier mass loss in the Arctic Canada South region is more closely linked to summer temperatures than winter precipitation at longer timescales (Barrand et al., 2017; Sharp et al., 2011) so mass losses will likely continue throughout the 21st century.

3.4 Wind speed related indices

3.4.1 Observed wind speed variability and trends

There are relatively few long-term homogeneous wind speed datasets suitable for analysis of trends in Nunavik and Nunatsiavut. One of the reasons for this is that wind speed observations are very sensitive to changes in measurement location, anemometer height, and/or physical characteristics of a measuring site (for example the location and height of nearby buildings and trees). Information on wind speed over the region was obtained from the CFSR reanalysis product (Saha et al., 2010). Three other reanalysis products were also considered, namely ERA-Interim, MERRA-2 and JRA-55 (Kobayashi et al., 2015). The choice of CFSR was mostly based on the differences (biases) in the average wind speed over 1980–2004 between *in situ* measurements at 11 stations (see Figure 26) and corresponding reanalysis grid tiles. Indeed, when considering the distribution of 11 bias values for each reanalysis, CFSR presents the smallest absolute values for the extreme low, median and extreme high biases. However, as shown in Figure 26 described later, CFSR wind speed data present a marked distinct regime in the northern area (approximately north-west of the imaginary line between Umiujaq and Tasiujaq), and all of the 11 evaluation stations were located outside of this area. Other reanalyses also present (different) marked regime shifts across Nunavik and Nunatsiavut but the reasons for this are unclear.

Mean annual wind speed values at 10 m height during the 1980–2004 period (Figure 26) range from 2.8 to 5.2 m/s (~10 to 19 km/h) over the station data in the region consistent with the Wan et al. (2010) results from homogenized station data. The largest mean wind speed values are located over the Ungava Peninsula and along the Nunatsiavut coast where Hopedale and Cartwright have mean annual wind speeds exceeding 5 m/s (> ~20 km/h). Wan et al. (2010) evaluated wind speed trends over Canada after an extensive effort to homogenize records for shifts in station location and changes in anemometer heights. Their analysis included several stations in or near the region (Hopedale, Goose Bay, Cartwright, Schefferville, Kuujjuarapik, and Kuujjuaq) and the results showed a small but statistically significant decrease in wind speeds over the region of about 1 km/h over the period 1953–2006. Decreasing wind speed, warmer winter temperature and decreasing numbers of days with extreme wind chill over the region were reported by Mekis et al. (2015). However, local knowledge from the region does not support the observation of declining wind speed. The synthesis of local observations of environmental change in Nunavik presented in Cuerrier et al. (2015) states that 4 of the 5 surveyed communities report stronger winds. Changing wind speed patterns and changes to the timing of strong winds through the year were also frequently noted by survey participants. Future work is needed to better assess the contradictory results between traditional knowledge and scientific knowledge in this domain and also to evaluate the representativeness of existing monitoring stations.

3.4.2 Projected change in wind speed

The wind scenarios (Figure 27) show only weak changes in annual averaged daily maximum 10-meter wind speeds over periods H50 and H85 for RCP 4.5, with a lack of consensus among models on the sign of the projected change for large portions of Nunavik and Nunatsiavut except for the northern part of Nunavik where wind speeds are projected to increase slightly. Small projected changes in maximum wind speed are projected for H85 under emissions scenario RCP 8.5 with models in agreement for increasing maximum wind speeds over much of Nunavik of ~0.20 to 0.42 m/s (~1.5 km/hr; Table 4). This contrasts with Nunatsiavut where the models do not agree on the sign of projected change (Figure 27). Very few studies have assessed projected wind speed changes at either the pan-Arctic scale or over Nunavik and Nunatsiavut due to the coarse spatial resolution of CMIP5 models (Ouranos, 2015). Kulkarni and Huang (2014) show increasing trends for the end of the century for winter wind speeds while summer wind speed is generally projected to decrease. Results from the Kulkarni and Huang (2014) study for the most southern areas Nunavik and Nunatsiavut remain difficult to compare with the current update's indices as seasonal analyses for wind speed were not produced.

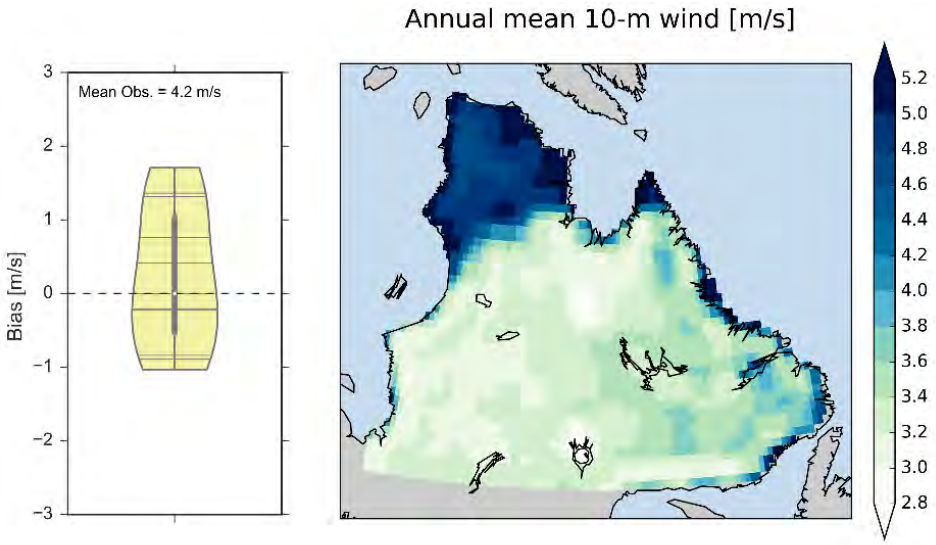

Figure 26: Climate reference map for the annual mean 10 m wind speed for the period 1980–2004 obtained from CFSR. The violin plot shows biases in grid points close to 11 surface stations situated inside the domain. Mean Obs. represents the regional mean of station indices values.

Table 4: Summary of the projected climate changes for indices related to wind speed for the H50 period (the first line) and the H85 period (the second line). The lower bond of the interval of values presented in the table corresponds to RCPs 4.5 (first value) and 8.5 (last value).

Climate indices	Nunavik		Nunatsiavut	
	Projected Change **H50: RCP4.5 to RCP8.5** **H85: RCP4.5 to RCP8.5**	**Comments**	**Projected Change** **H50: RCP4.5 to RCP8.5** **H85: RCP4.5 to RCP8.5**	**Comments**
Wind average maximum speed (m/s) **RCP 4.5 and 8.5**	+0.02 to +0.26 +0.02 to +0.42	Largest change over the Hudson Bay's and Hudson Strait coasts and over the Ungava Peninsula. Some models show changes of opposite sign.	0 to +0.06 -0.06 to +0.22	Change is more heterogeneous than Nunavik with no model consensus for the direction of change.

3.5 Sea ice cover and related indices

3.5.1 Observed sea ice cover variability and trends

The 2012 IRIS-4 report (Allard and Lemay, 2012) provided a comprehensive review of the historical sea ice data available at that time, which together with local knowledge described a shortening of the ice-covered season, and thinning of seasonal ice with adverse effects on safe access to territory and its resources (Furgal and Tremblay, 2010). Updated information on sea ice trends in coastal waters around Nunavik and Nunatsiavut was obtained through analysis of the Canadian Ice Service Digital Archive (CISDA) weekly ice charts (Tivy et al., 2011) for a series of polygons covering approximately 2° latitude along the coasts of Nunatsiavut and Nunavik (Figure 28). The CIS ice reconnaissance program covers the June-November shipping season in all the polygons except southern Nunatsiavut where the

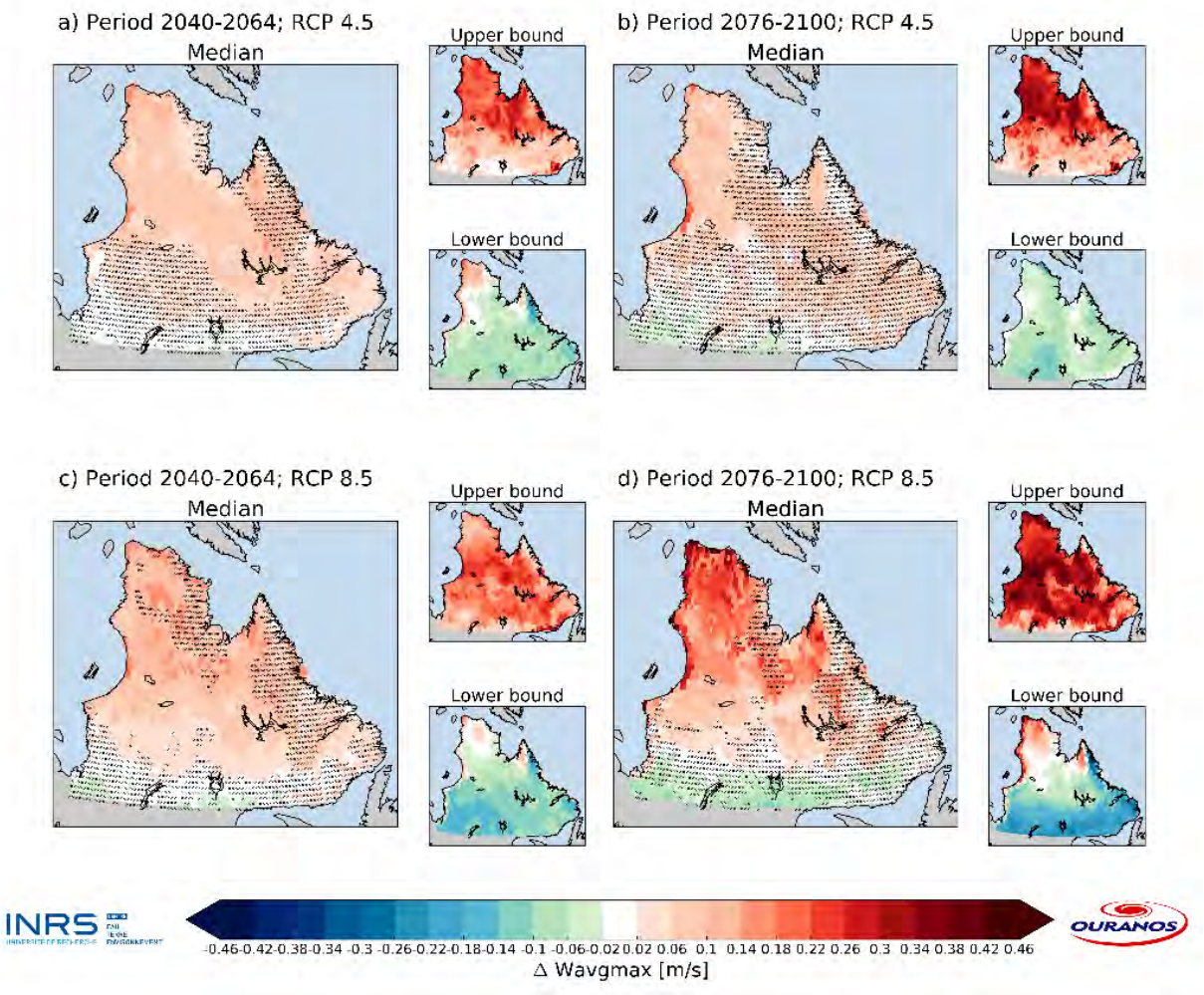

Figure 27: Same as Figure 8 for projected change in annual average of the daily maximum 10-meter wind speed (m/s).

observing program only occurs during winter between January and March. Time series of shipping season mean ice area for all ice types were computed over weeks 25–47 following Mudryk et al. (2018), which corresponds approximately to the period of June 18 to November 19. These data show significant reductions of ice-covered area (Figure 28) including ~30 % decrease per decade over the Hudson Strait and northern Nunatsiavut regions. These trends show the largest decrease of sea ice in Canadian waters based on updated regional ice cover trends provided in Mudryk et al. (2018). The Nunatsiavut South region showed no trend in winter ice area. In the two eastern Hudson Bay regions, significant trends in ice area were not observed similar to results presented by Mudryk et al. (2018). These two regions, particularly the southern one, exhibit several high ice cover years over the past decade, most notably 2004 and 2015 which offset negative trends in summer ice cover observed in adjacent areas. The magnitude of the 2004 and 2015 ice area anomalies was likely influenced by colder than normal spring/summer air temperatures in the region.

More insight into the spatial pattern of ice cover trends was obtained from passive microwave satellite monthly ice concentration data (Peng et al., 2013), which have the advantage of being available year-round from 1979. Trend in monthly sea ice concentration over 1979-2016 was investigated from linear regression analysis of the Meier et al. (2017) ice concentration data derived from the GSFC NASA Team/Bootstrap method (Figure 29). The results show significant decreases in spring (June-July) and fall (November-December) sea ice concentration in most coastal waters around Nunavik and Nunatsiavut with the largest decreases in Hudson Strait, Ungava Bay and northern Nunatsiavut zones consistent with the results obtained with the CISDA dataset. The passive microwave trends exhibited a large gradient over

eastern Hudson Bay with the largest ice decreases observed closer to the coast. This gradient may explain the lack of significance in the trend results obtained with the CISDA dataset over the eastern Hudson Bay regions where ice area variation is averaged over relatively large areas. This gradient in ice concentration trends over eastern Hudson Bay is a feature in the projected changes in ice concentration simulated by Joly et al. (2011) and also in projected changes in the safe period for over-ice travel (Figure 34).

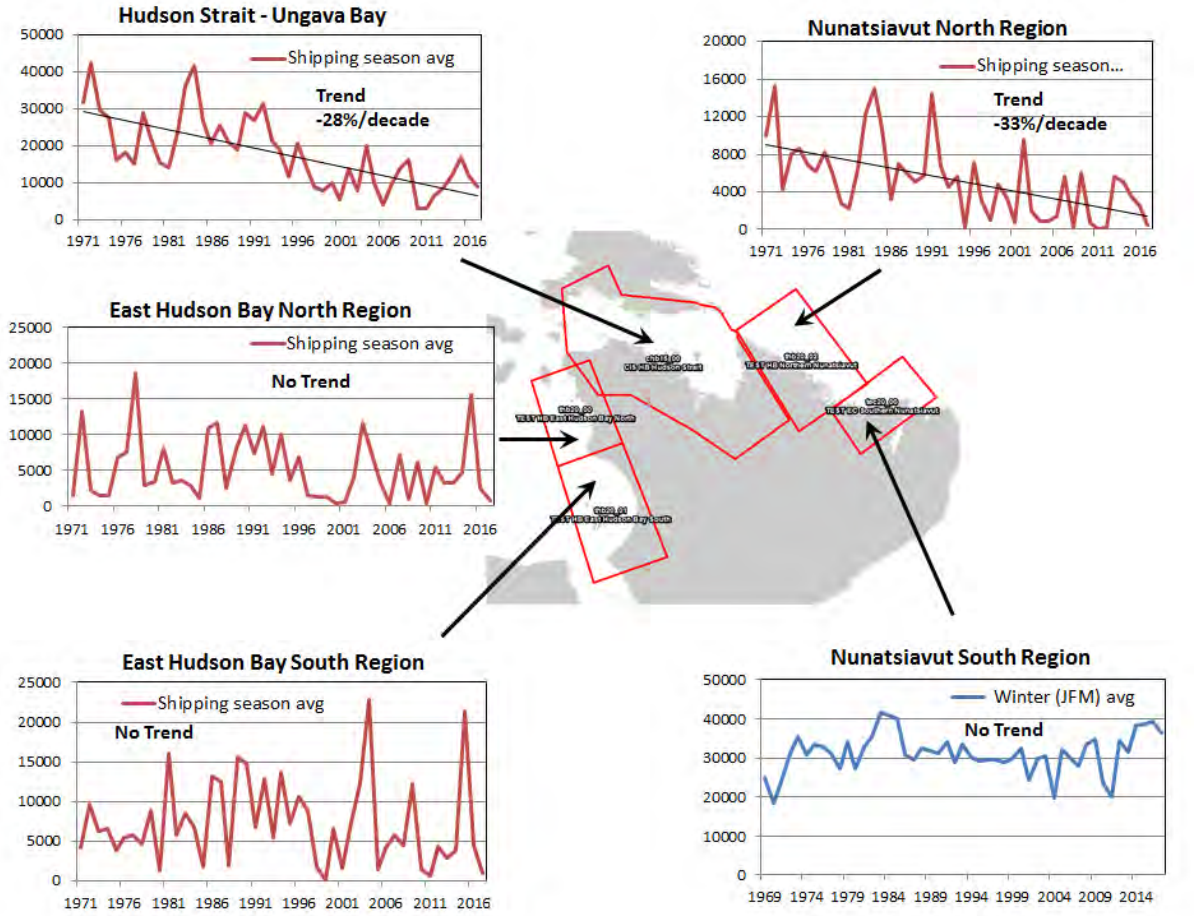

Figure 28: Time series of shipping season (June 18-November 19) average ice area (km^2) for all ice types (red lines) in coastal regions of Nunavik and Nunatsiavut from the Canadian Ice Service historical weekly ice chart database. Winter (January-March) ice area for all ice types (blue line) is shown for the Nunatsiavut South region as the ice reconnaissance program is only carried out in winter months over more southerly waters. The trends were computed from least-squares regression and the trend expressed as the areal change per decade with respect to the mean ice area for 1981–2010.

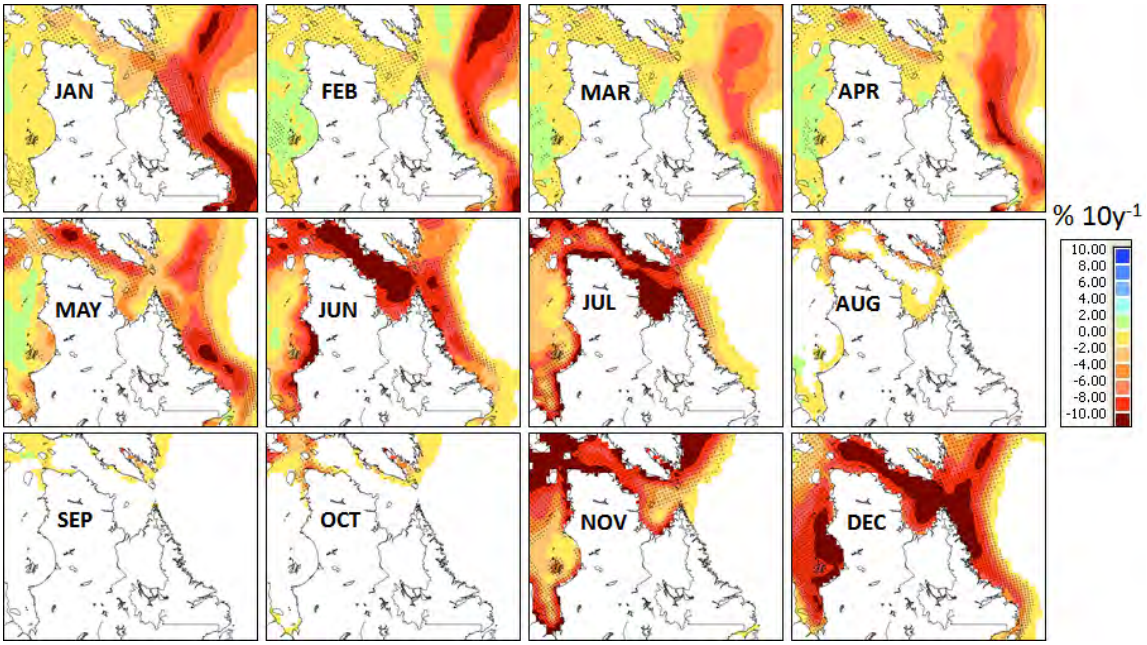

Figure 29: 1979–2016 trend (% per decade) in monthly average ice concentration from the merged Goddard passive microwave dataset (Meier et al., 2017). Stippling indicates grid points with locally significant (0.05 level) trends.

3.5.2 Recent climatology of the period for safe travel on coastal sea ice

As part of this update, an analysis was carried out to estimate the stability of the coastal fast ice zone with respect to wave-induced break-up over the coastal regions of eastern Hudson Bay, Hudson Strait and Ungava Bay. The index derived from this research project is termed the "safe period", and is defined as the longest anticipated time period during which sea ice is not broken up by waves. The choice of the domain used in this analysis is based on the research being carried out at UQAR-ISMER in collaboration with the Ministère des Transports du Québec to better protect maritime infrastructure in Nunavik. The Nunatsiavut coastal region could not be included in this experiment as it is located outside the sea ice model domain. The period for safe travel includes bias corrected wind scenarios used to simulate waves from the CFSR model (Saha et al., 2010), the simulation of sea ice cover with the coupled ice-ocean model (Senneville and St-Onge-Drouin, 2013; Saucier et al., 2004), and the use of a third generation spectral wave model that includes wave-ice interactions (Boutin et al., 2018; WW3 Develop. Group, 2016; Williams et al., 2013). The wave climate is simulated with a closed boundary at the eastern end of the domain, near the mouth of Hudson Strait. The bias imparted to the omission of waves generated outside the domain and entering through this boundary is estimated over the domain, to show the regional spreading of the error within the Hudson Strait, and at a station position along the coast (station located offshore of Quaqtaq). The coupled ice-ocean model used (Senneville and St-Onge-Drouin, 2013; Saucier et al., 2004) was recently validated against CIS ice charts as part of a project funded by Ministère des Transports du Québec. Validation of wind results from the CFSR for both marine and continental areas remains a challenge as there are only a few climate stations have reliable information (11 stations over the region) that can be used and these stations are mostly located in the south-center of the region.

Model results for the recent past period 1982–2004 show that the typical sea ice season duration is approximately 255 days over the Hudson Bay and slightly less over Ungava Bay. The period over which the simulated ice thickness is sufficient for safe travel is 180 to 200 days/year along the Hudson Bay coasts and 180 to 240 days/year over the Ungava Bay (Figure 30a). For coastal areas of Nunavik and Nunatsiavut included in the model domain, the longest safe period is located in the southern region of the Ungava Bay where ice thicknesses of more than 3 m are simulated (Figure 30b). The shortest safe ice travel period is simulated around the Nastapoka Islands (Hudson Bay's Nunavik coasts, Umiujaq and Inukjuak) and in the Hudson Strait near Salluit and Deception Bay.

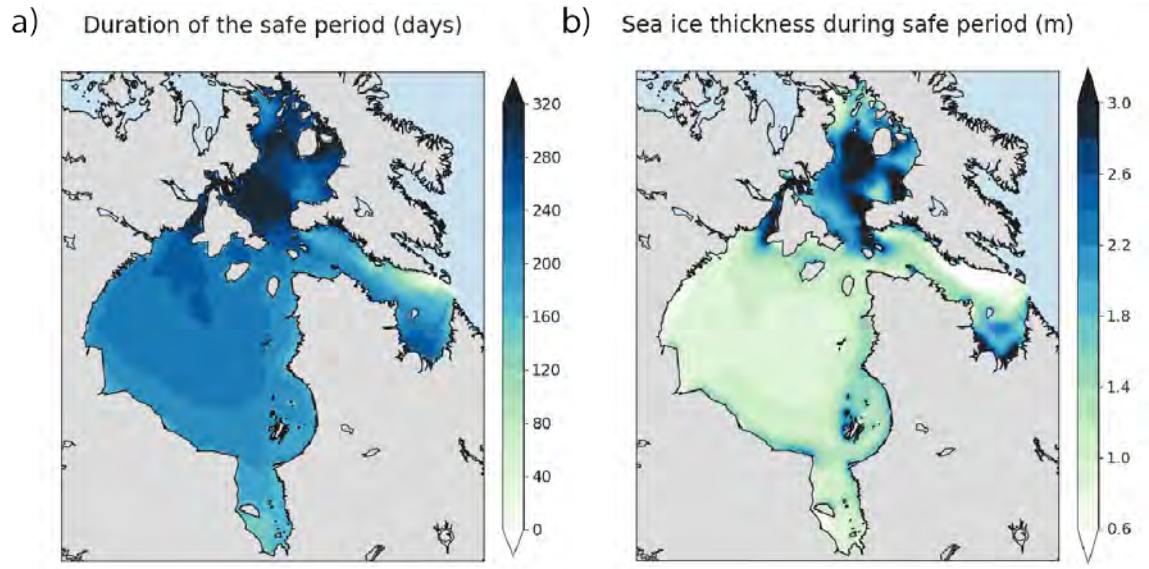

Figure 30: 1982–2004 reference climate for a) the duration of the safe period, and b) the average sea-ice thickness during the safe period.

3.5.3 Projected change in sea ice

The sea ice model used in the climate change scenarios projections is based on Senneville and St-Onge-Drouin (2013) and Saucier et al. (2004) and covers the region of the Hudson Bay, Hudson Strait, Ungava Bay as well as of the Foxe Basin. Sea ice projections for the Nunatsiavut region remains a knowledge gap. The projected changes for sea ice as well as for wave heights and safe period for travel on ice (discussed in sections 3.7.2) are based on two CRCM runs (de Elia and Côté, 2010) driven by ECHAM5 and CGCM3.1/t47 GCM for the SRES A2 emission scenario that has comparable radiative forcing to RCP 8.5 and three global climate model simulations that are using RCP 8.5.

Figure 31 shows the mean projected changes for ice onset dates and ice melt dates over the Hudson Bay, and the Ungava Bay. The mean projected onset and melt dates correspond to the dates when median sea-ice concentration crosses 30 % (Joly et al., 2011). The ice onset date is projected to change by up to 64 days later for H85 with ice melt date projected to occur earlier in the season by a similar magnitude. A seasonal ice cover is projected to persist over the Hudson Bay and Ungava Bay domain throughout this century (Figure 32) consistent with results from other studies like Hu and Myers (2014). However, the projected decreases in its extent and duration will have profound impacts on the natural and human systems in the region.

3.5.4 Projected changes for safe travel on the ice

The development of scenarios of projected changes in the period of ice safe for travel also required developing scenarios for changes in winds, waves and ice cover over the region.

Annual mean significant wave heights are projected to increase between about 0.06 to 0.2 m for H50 period and between about 0.1 to ≥0.3 m for H85 period (Figure 33). The projected changes follow a west-to-east pattern over the greater Hudson Bay area with the largest increases near Nunavik's coastal regions. The impact of declining ice cover (and thickness) and increasing wave heights on the start and end dates of the period safe for ice travel is shown in Figure 34. Large decreases in the duration of the safe period of about 3–4 months are projected for H85 and RCP 8.5 over much of the Nunavik coastline in response to delayed ice formation and earlier melt. The projected changes are relatively symmetric for the onset and melt periods with changes of about 1.5 to 2 months in each case, and the largest changes indicated over the Hudson Bay Nunavik coasts. Hunters in the communities of Nunavik and Nunatsiavut are already experiencing the impacts of declining ice cover (Ford et al., 2016; Ford et al., 2010; Communities of Ivujivik et al., 2005; Communities of Labrador et al., 2005), and the above results suggest a significant worsening of ice travel safety over the rest of the century if greenhouse gas emissions follow RCP 8.5.

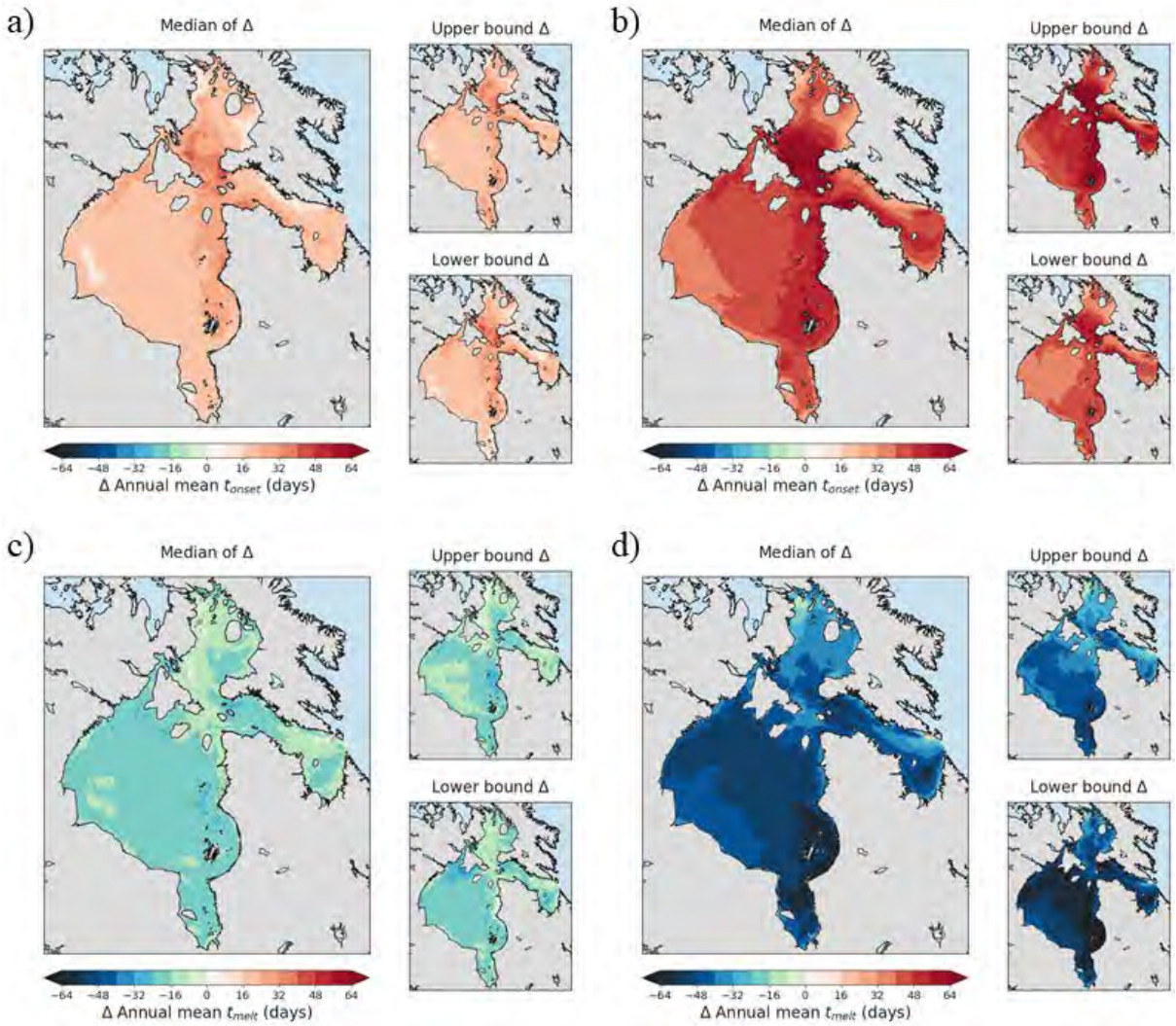

Figure 31: Climate-mean differences (Δ) between the future periods and the reference period (1982–2004) for ice onset date (a and b) and for ice melt date (c and d). The Δ are shown for the periods 2040–2064 (a and c) and 2076–2100 (b and d), which refer to the results drawn from the simulations forced with the SRES-A2 greenhouse gas emission scenario. The central map of each panel shows the median of the simulated differences at each grid-points. The small, secondary maps give an indication of the dispersion of the projected changes by the ensemble of models. The upper bound (Δ) shows the simulation with the greatest mean differences over the domain, while the lower bound (Δ), the smallest ones.

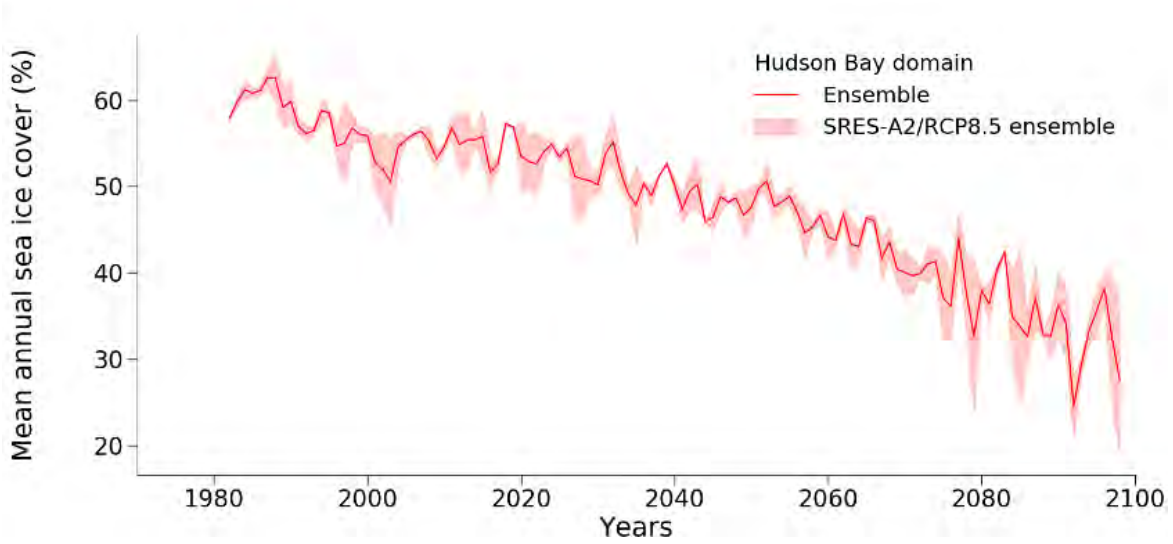

Figure 32: Time evolution of mean annual ice cover over the Hudson Bay domain. The red zone corresponds to the spread of the ensemble.

3.6 River and lake ice cover related indices

3.6.1 Observed river and lake ice cover trends and variability

There is very little new published information about ice cover trends on lakes and rivers since the 2012 IRIS-4 report (Allard and Lemay, 2012) which provided evidence of trends to earlier ice break-up and later freeze-up across the region, along with community-based evidence of decreasing ice cover duration and deteriorating stability for over-ice transport. Studies by Brown and Duguay (2012) and Du et al. (2015) evaluated some of the recent satellite products for lake ice cover monitoring including MODIS, AMSR-E and the Interactive Multisensor Snow and Ice Mapping System (IMS). In general, the different products agree well with each other but the series are too short to provide insights into long-term trends. Analysis of daily lake ice cover over Nunavik with the IMS-4km snow and ice analysis showed no trends for ice-on/off dates as well as for average annual ice cover over the 2004–2017 period (not shown).

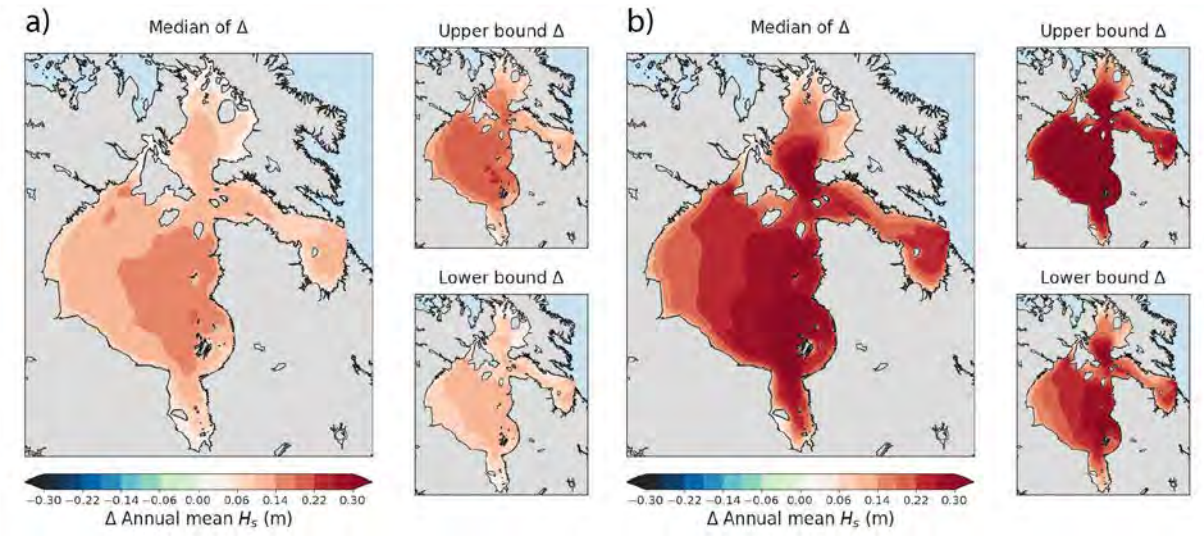

Figure 33: Projected change in annual mean significant wave height (m) following Figure 31.

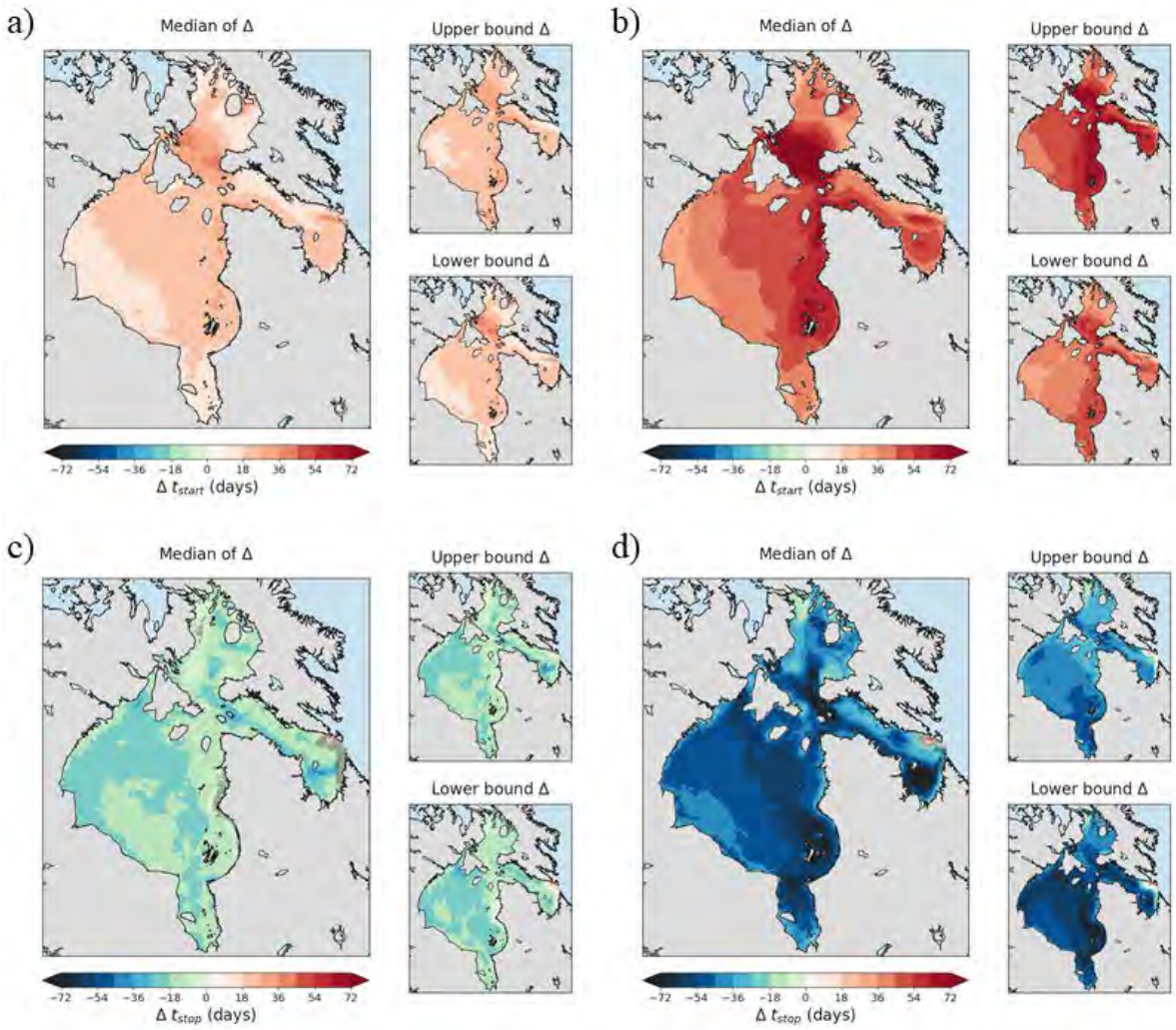

Figure 34: Same as Figure 33 for projected change (days) in the start (a and b) and end dates (c and d) of the safe period for ice travel.

Community-based monitoring of the period that ice is safe to cross between Happy Valley-Goose Bay, NL and Mud Lake, NL just south of Nunatsiavut (Figure 35a) shows evidence of a significant (0.05 level) decrease in the period of ice safe for travel of ~4 days/decade since the mid-1970s, with duration closely linked to mean winter air temperatures (Figure 35b). To provide further insight into trends in ice thickness and ice cover over Nunavik and Nunatsiavut, a 1-D ice growth model with a varying surface snow layer following Brown and Coté (1992) was driven with ERA-interim 6-hourly temperature and precipitation over the 1979/80–2015/16 period. This model is a simplified version of the CliMO model used by Brown and Duguay (2012) which assumes shallow water (no heat flux from the water column) and ignores white ice formation. The simulated ice cover from the model at the nearest grid point to Happy Valley-Goose Bay/Mud Lake, Newfoundland and Labrador is shown in Figure 35c assuming a 10-cm thickness threshold for safe ice travel. The model overestimates mean ice cover duration by about 20 days, but does a reasonable job of capturing the observed variability (r=0.82), with the exception of the low ice cover year in 1982, and correctly reproduces the observed trend. The ice cover simulation shows ice thickness trends of -2 to -6 cm/decade over much of Nunavik and Nunatsiavut (Figure 36a) but the local trends are for the most part not statistically significant due to the variability generated by an annually varying snow cover that exerts a dominant role in ice growth rates (Brown and Coté, 1992; Andrews, 1962). In contrast, simulated ice cover duration (Figure 36b) shows widespread locally significant trends of -4 to

-10 days/decade due to the strong link to air temperature as seen at the Mud Lake river crossing site. Analysis of ice-onset and ice-off dates (not shown) revealed stronger and more widespread locally significant trends in delayed ice-onset which is consistent with the observed warming trends over the region which are largest in the October-December period (Rapaic et al., 2015; Figure 13).

The above evidence of widespread decreases in ice cover is not observed across all communities. Cuerrier et al. (2015) carried out a survey of environmental change at three Nunavik communities (Kangiqsualujjuaq, Kangiqsujuaq, and Umiujaq) and they only found a broad consensus for earlier break-up. As noted earlier, local factors such as snow accumulation exert an important role in ice growth through its insulating effect, and two of the three communities reported decreasing trends in snow cover that may be offsetting the effect of a shorter ice growth season. Other communities in Nunavik and Nunatsiavut report thinner sea ice, less multiyear sea ice, later freeze-up and earlier break-up (Rapinski et al., 2017; Ford et al., 2016; Ford et al., 2010; Communities of Inuvik et al., 2005; Communities of Labrador et al., 2005).

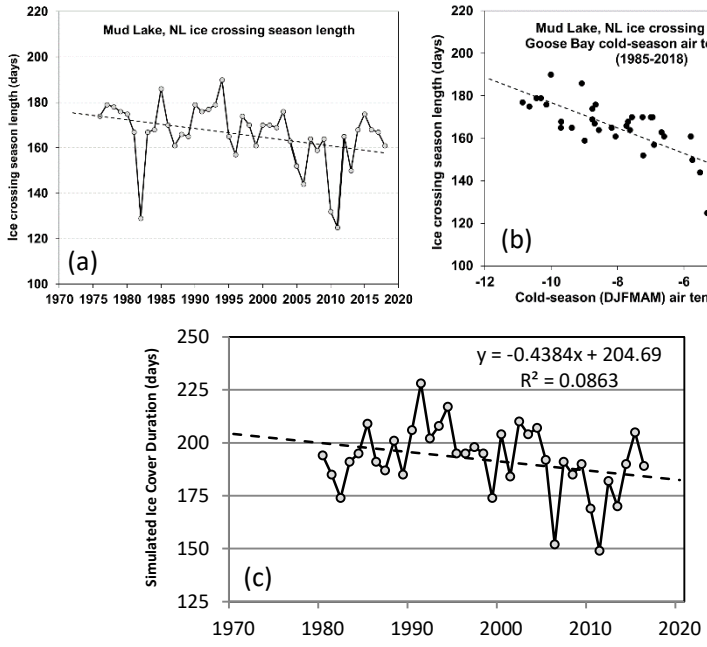

Figure 35: a) Time series of the ice-crossing season length (days) at Mud Lake, NL (just south of Nunatsiavut). Ice-crossing season length was calculated as the period between the dates of the first and last recorded crossings. The data were collected by members of the community of Mud Lake and collated from 2015–2016 ice observation survey by Sikumiut Ltd. b) Crossing season length is closely correlated with cold-season air temperature recorded at Goose Bay. c) ERA-interim simulated ice cover duration for ice thickness ≥ 10 cm at the grid point located closest to Mud Lake. Mud Lake graphs provided by R. Way, Labrador Institute, Memorial University of Newfoundland.

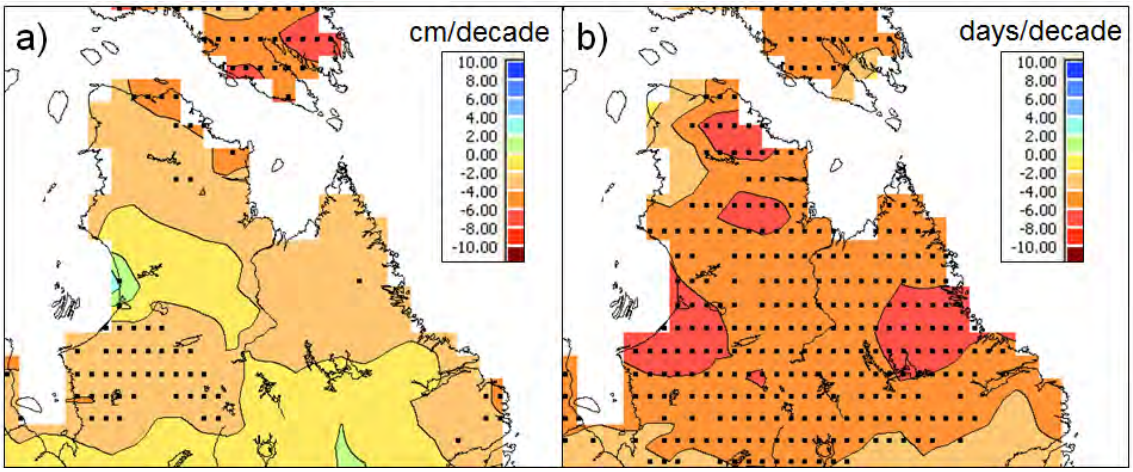

Figure 36: ERA-interim simulated ice cover trends for shallow fresh water bodies over the 1979/80–2015/16 period using a 1-D ice growth model with surface snow layer following Brown and Coté (1992): (a) annual maximum ice thickness (cm/decade), and (b) ice cover duration (days/decade). Black squares denote grid points with significant trends at the 0.05 level.

Table 5: Projected change in wave and sea ice related variables from the ice stability analysis based on the SRES A2 and RCP 8.5 scenarios. The lower and upper bounds are for H50 and H85 respectively.

Climate indices	Nunavik		Nunatsiavut	
	Projected Change	**Comments**	**Projected Change**	**Comments**
Annual mean significant wave height (m) **SRES A2**	+ 0.1 to +0.22 +0.06 to ≥0.3	Spatial gradient showing largest changes near Nunavik coasts between Akulivik and Umiujaq.	NA	NA
Ice onset date (days)	+16 to ≥64	Spatial gradient showing largest changes near Nunavik coasts between Akulivik and Inukjuak. Hot spot projected in Hudson Strait near Salluit and Deception Bay.	NA	NA
Ice melt onset (days)	-16 to ≤-64	Most important changes in the Nastapoka Islands region.	NA	NA
Duration of the safe period (days)	0 to -136	Largest change along Nunavik's coasts and over Ungava Bay.	NA	NA
Ice thickness during safe period (m)	-0.2 to ≤-1.6	Ice thickness change along the Hudson Bay coast of Nunavik with largest changes over southern Ungava Bay.	NA	NA

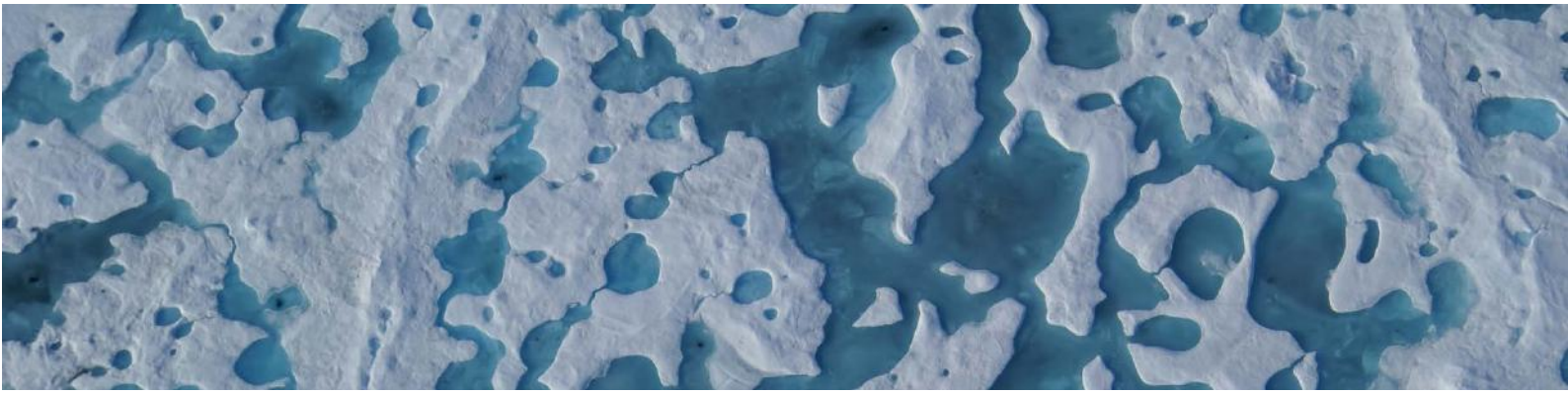

4. Summary and conclusions

This update of the IRIS-4 report (Allard and Lemay, 2012) provides further evidence of continued long-term warming over the region of ~1.0 °C/100y since 1850, with the period since ~1970-today characterized by pronounced multi-decadal variability related to a range of climate forcing mechanisms including salinity anomalies, volcanic activity, and anomalies in atmospheric and oceanic circulation. The recent 1987–2016 period analyzed here is characterized by stronger warming in winter (1.5-2.0 °C/decade) with the magnitude of the warming trend increasing northward consistent with poleward amplification of global warming. The recent period is also characterized by widespread significant summer warming of ~0.5 °C/decade associated with a marked increase in the period with above-freezing temperature by 5–8 days/decade over coastal areas where most of the communities of Nunavik and Nunatsiavut are located. Both natural and anthropogenic forcing were determined to be significant factors in explaining the observed rapid warming over the past two decades (Way and Viau, 2014). The observed warming is driving a wide range of environmental changes including declining snowfall, shorter periods of snow and ice cover, thinner and less safe ice, rapid shrub growth, permafrost warming and thawing, and the rapid thinning and shrinkage of mountain glaciers. These changes are consistent with pan-Arctic observations of environmental changes and a direct response to the pronounced warming observed over northern latitudes (AMAP 2017a; Derksen et al., 2012). These changes are expected to continue in response to further projected warming. The update also provides evidence of a 2–3 % per decade regional increase in observed precipitation from climate station records since 1950. This increase in precipitation is also observed at the pan-Arctic scale from multiple datasets along with concurrent reductions in the solid fraction of precipitation (AMAP, 2017a).

Climate change scenarios developed for this update were more advanced than those used in the previous assessment (Allard and Lemay, 2012) with respect to the following aspects:

(1) the scenarios were based on a larger number of model simulations, and a larger number of driving GCMs and RCMs;
(2) two emission scenarios were used to provide some guidance on the sensitivity of the regional climate change to efforts to reduce future greenhouse gas emissions; and
(3) climate extremes scenarios were included for variables such as warm and wet days.

The results from these scenarios project a long-term warming trend throughout this century with a 5–7 °C projected warming of mean annual air temperature by 2085 for the two emission scenarios RCP 4.5 and RCP 8.5. A 4° C warming of the mean annual air temperature is projected by 2050 and is insensitive to emission scenarios (is a response to the "locked-in warming" from the cumulative carbon emissions in the atmosphere). The projected warming is strongest in winter and over northern parts of Nunavik and Nunatsiavut, but the projected changes in important temperature sensitive indices such as summer season length and annual extreme air temperatures are relatively uniform over the region. Projected changes in freezing degree days, which exerts a strong control on maximum ice growth, show large declines over the northernmost areas of the region.

Due to the strong natural climate variability of the region, the future path of air temperature will include periods of relative warming or cooling around the long-term warming as described in AMAP (2017c). A key question for the region, particularly for Nunatsiavut, is whether future warming has the potential to modify the Atlantic Meridional Overturning Circulation (AMOC), or the strength and phase of the AO-NAO which both influence the climate of the region. There is a body of observational and model-based evidence linking a weakening of the AMOC to global warming, and some climate models simulate rapid cooling events linked to collapse or disruption of the AMOC. There is currently insufficient information to provide any guidance on the risk and implications of such cooling events for Nunavik and Nunatsiavut. This is also the case for potential shifts in AO-NAO phase from a weaker polar vortex in response to declining Arctic sea ice. Further research on these topics and the potential climate consequences for Nunavik and Nunatsiavut are recommended in light of the importance of AMOC and AO-NAO to the climate of the region.

This update included new analysis of projected warming impacts on the coastal wave and ice regime of Nunavik. This was previously highlighted as an important gap in the context of coastal community and marine infrastructure adaptation needs. The analysis revealed that coastal wave and ice dynamics are sensitive to projected warming with reductions in the safe period for over-ice travel in Nunavik coastal areas by ~30 days for 2050, but by more than 100 days for 2085 under the SRES-A2 scenario. Projected reductions are largest along the Hudson Bay coast of Nunavik. The simulated high sensitivity of the safe period for ice travel to warming will be a major concern for hunters in the region who are already experiencing adverse impacts from declining ice cover. However, it is important to note that a considerable knowledge gap persists over Nunatsiavut where model simulations have not been performed for these ice travel metrics. Additional research is needed to characterize the future evolution of the safe ice travel period across Nunavik and Nunatsiavut and particularly in Nunatsiavut given the region's reliance on ice travel routes (Riedlsperger, 2013).

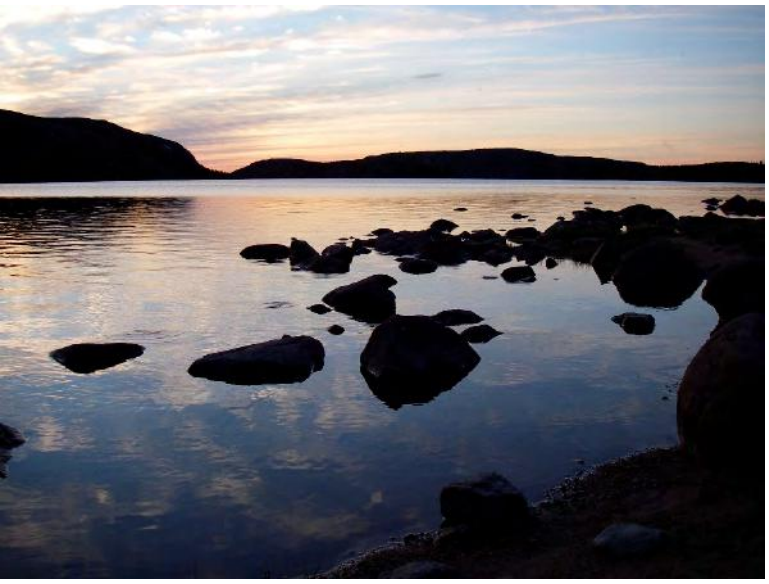

Extremes related to air temperature, precipitation and wind speed are also assessed in the current update. Warm and wet extremes are projected to occur more frequently and with more intensity in the future, consistent with pan-Arctic results from the CMIP5 ensemble presented in AMAP (2017c) report. Projected increases in extreme precipitation are a response to the increasing moisture-holding capacity of warming air parcels (Laîné et al., 2014). However, there is evidence that most climate models still underestimate the sensitivity of extreme precipitation to warming air temperatures over mid latitudes and this could also be the case for higher latitudes as well (IPCC, 2013). Finally, for wind speed, annual average daily maximum 10-m wind speeds are projected to show a small increase over most of the region in RCP 8.5 (H85 period) in most climate simulations.

From the previous IRIS-4 report (Allard and Lemay, 2012), it was highlighted that assessing climate variability, trends and changes in regions where climate observations are sparse and often incomplete is a clear challenge. These same challenges remain in regards to assessing many of the climate indices presented here, and this is especially true for wind, wave and ice-related indices. For instance, few snow, wind and wave observational station data are available in the region which clearly needs a better distribution and a larger number of monitoring stations. Observations are essential for monitoring long-term changes, for contributing to improved understanding of climate processes and interactions, and for the evaluation of climate and process models. A better network of stations would also allow better comparisons of precipitation and snow cover products and would help improve our understanding of the various processes and interactions between the climate features and to a larger degree to improve climate model experiments. A recent University-led initiative

(Coastal Labrador Climate and Weather Monitoring Program) established six automatic weather stations in coastal Labrador including in Nunatsiavut (communities of Postville and Rigolet). Near real-time climate information provided by these stations (www.smartatlantic.ca) is now being widely used by Labrador community members but is coincident with weather station closures and sensor reductions by Environment Canada and its partners elsewhere in Labrador. This contrast highlights the challenge of assessing climate trends across Nunavik and Nunatsiavut and the clear need for maintaining a robust climate observing network in northern Canada.

As noted throughout this update, indigenous and non-indigenous communities in Nunavik and Nunatsiavut are reliant on local environmental conditions for safe and reliable access to traditionally used territories. The observed changes in ice and snow conditions and other related environmental components have very likely had negative impacts on the physical and mental health of people in the region (Ford et al., 2017; Cunsolo Willox et al., 2015; Cunsolo Willox et al., 2013) and model simulations of continued warming and declining snow and ice cover suggest that these impacts may be exacerbated in the future. It is important that more work be done to better integrate climatological observations and projections with local knowledge for use in community and regional-level planning. Further, access to meaningful climate information will support building local capacity and will help ensure that local vulnerabilities can be evaluated and responded to in a timely manner.

References

Allard, M., and Lemay, M. (2012). Nunavik and Nunatsiavut: From Science to Policy. An Integrated Regional Impact Study (IRIS) of climate change and modernization. ArcticNet Inc, Québec City, Canada, 303pp.

AMAP. 2017a. Snow, Water, Ice and Permafrost in the Arctic (SWIPA) 2017. Retrieved from https://www.amap.no/documents/doc/snow-water-ice-and-permafrost-in-the-arctic-swipa-2017/1610.

AMAP. 2017b. Adaptation Actions for a Changing Arctic: Perspectives from the Barents Area. Arctic Monitoring and Assessment Programme (AMAP), Oslo, Norway, xiv, 267pp.

AMAP. 2017c. Adaptation Actions for a Changing Arctic: Perspectives from the Baffin Bay and Davis Strait Area. Arctic Monitoring and Assessment Programme (AMAP), Oslo, Norway, xiv, 354pp.

AMAP. 2017d. Adaptation Actions for a Changing Arctic: Perspectives from the Bering Chukchi and Beaufort Region. Arctic Monitoring and Assessment Programme (AMAP), Oslo, Norway, xiv, 255pp.

Andrews, J.T. 1962. Variability of lake ice growth and quality in the Schefferville Region, Central Labrador-Ungava. Journal of Glaciology, 4, 337–347.

Angers-Blondin, S., and Boudreau, S. 2017. Expansion dynamics and performance of the dwarf shrub *Empetrum hermaphroditum* (Ericaceae) on a subarctic sand dune system, Nunavik (Canada). Arctic, Antarctic, and Alpine Research, 49, 201–211.

Barnes, E.A., and Screen, J.A. 2015. The impact of Arctic warming on the midlatitude jet-stream: Can it? Has it? Will it? Wiley Interdisciplinary Reviews: Climate Change, 6, 277-286.

Barrand, N.E., Way, R.G., Bell, T., and Sharp, M.J. 2017. Recent changes in area and thickness of Torngat Mountain glaciers (northern Labrador, Canada). The Cryosphere, 11, 157-168.

Bell, T., and Brown, T.M. 2018. From Science to Policy in the Eastern Canadian Arctic: An Integrated Regional Impact Study (IRIS) of Climate Change and Modernization. ArcticNet Inc, Québec City, Canada, 560pp.

Bokhorst, S., Pedersen, S.H., Brucker, L., Anisimov, O., Bjerke, J.W., Brown, R.D., Ehrich, D.E., Richard, L.H., Heilig, A., Ingvander, S., Johansson, C., Johansson, M., Jónsdóttir, I.S., Inga, N., Luojus, K., Macelloni, G., Mariash, H., McLennan, D., Rosqvist, G.N., Sato, A., Savela, H., Schneebeli, M., Sokolov, A., Sokratov, S.A., Terzago, S., Vikhamar-Schuler, D., Williamson, S., Qiu, Y., and Callaghan, T.V. 2016. Changing Arctic snow cover: A review of recent developments and assessment of future needs for observations, modeling, and impacts. Ambio, 45, 516–537.

Bosilovich, M.G., Lucchesi, R., and Suarez, M. 2016. MERRA-2: File Specification. GMAO Office Note No. 9 (Version 1.1), 73 pp. https://gmao.gsfc.nasa.gov/pubs/docs/Bosilovich785.pdf.

Bouchard, F., Francus, P., Pienitz, R., Laurion, I., and Feyte, S. 2014. Subarctic Thermokarst Ponds: Investigating Recent Landscape Evolution and Sediment Dynamics in Thawed Permafrost of Northern Québec (Canada). Arctic, Antarctic, and Alpine Research, 46, 251–271.

Boutin, G., Ardhuin, F., Dumont, D., Sévigny, C., Girard-Ardhuin, F., and Accensi, M. 2018. Floe size effect on wave-ice interactions: Possible effects, implementation in wave model, and evaluation. Journal of Geophysical Research, 123, 4779-4805.

Brown, R.D., and Coté, P. 1992. Interannual variability of landfast ice thickness in the Canadian High Arctic, 1950-89. Arctic, 45, 273-284.

Brown, R., Derksen, C., and Wang, L. 2010. A multi-data set analysis of variability and change in Arctic spring snow cover extent, 1967–2008. Journal of Geophysical Research, 115, D16111.

Brown, L.C., and Duguay, C.R. 2012. Modelling Lake Ice Phenology with an Examination of Satellite-Detected Subgrid Cell Variability. Advances in Meteorology, 2012, 1–19.

Brown, R., Lemay, M., Allard, M., Barrand, N.E., Barrette, C., Bégin, Y., Bell, T., Bernier, M., Bleau, S., Chaumont, D., Dibike, Y., Frigon, A., Leblanc,

P., Paquin, D., Sharp, M.J., and Way, R. 2012. Climate variability and change in the Canadian Eastern Subarctic IRIS region (Nunavik and Nunatsiavut). In: Allard, M. and M. Lemay (Eds), Nunavik and Nunatsiavut: From science to policy. An Integrated Regional Impact Study (IRIS) of climate change and modernization. ArcticNet Inc., Québec City, Canada, p. 57-93.

Brown, R., Vikhamar-Schuler, D., Bulygina, O., Derksen, C., Luojus, K., Mudryk, L., Wang, L., and Yang, D. 2017. Arctic terrestrial snow cover. Chapter 3 in: Snow, Water, Ice and Permafrost in the Arctic (SWIPA) 2017, pp. 25–64. Arctic Monitoring and Assessment Programme (AMAP), Oslo, Norway.

Brown, R., Tapsoba, D., and Derksen, C. 2018. Evaluation of snow water equivalent datasets over the Saint-Maurice river basin region of southern Québec. Hydrological Processes, 32, 2748-2764.

Caesar, L., Rahmstorf, S., Robinson, A., Feulner, G., and Saba, V. 2018. Observed fingerprint of a weakening Atlantic Ocean overturning circulation. Nature, 556, 191-196.

Callaghan, T.V., Johansson, M., Brown, R.D., Groisman, P. Ya., Labba, N., Radionov, V., Bradley, R.S., Blangy, S., Bulygina, O.N., Christensen, T.R., Colman, J.E., Essery, R.L.H., Forbes, B.C., Forchhammer, M.C., Golubev, V.N., Honrath, R.E., Juday, G.P., Meshcherskaya, A.V., Phoenix, G.K., Pomeroy, J., Rautio, A., Robinson, D.A., Schmidt, N.M., Serreze, M.C., Shevchenko, V.P., Shiklomanov, A.I., Shmakin, A.B., Sköld, P., Sturm, M., Woo, M.-K., and Wood, E.F. 2011. Multiple Effects of Changes in Arctic Snow Cover. Ambio, 40, 32–45.

Cohen, J., Screen, J.A., Furtado, J.C., Barlow, M., Whittleston, D., Coumou, D., Francis, J., Dethloff, K., Entekhabi, D., Overland, J., and Jones, J. 2014. Recent Arctic amplification and extreme mid-latitude weather. Nature Geoscience, 7, 627-637.

Communities of Ivujivik, Puvirnituq and Kangiqsujuaq, Furgal, C., Nickels, S., Kativik Regional Government – Environment Department. 2005. Unikkaaqatigiit - Putting the Human Face on Climate Change: Perspectives from Nunavik. Joint publication of Inuit Tapiriit Kanatimi, Nasivvik Centre for Inuit Health and Changing Environments at Université Laval and the Ajunnginiq Centre at the National Aboriginal Health Organization. Ottawa, Canada, 20p.

Communities of Labrador, Furgal, C., Denniston, M., Murphy, F., Martin, D., Owens, S., Nickels, S., Moss-Davies, P. 2005. Unikkaaqatigiit – Putting the Human Face on Climate Change: Perspectives from Labrador. Joint publication of Inuit Tapiriit Kanatimi, Nasivvik Centre for Inuit Health and Changing Environments at Université Laval and the Ajunnginiq Centre at the National Aboriginal Health Organization. Ottawa, Canada, 54p.

Cuerrier, A., Brunet, N.D., Gérin-Lajoie, J., Downing, A., and Lévesque, E. 2015. The study of Inuit knowledge of climate change in Nunavik, Quebec: a mixed methods approach. Human Ecology, 43, 379-394.

Cunsolo Willox, A., Harper, S.L., Ford, J.D., Edge, V.L., Landman, K., Houle, K., Blake, S., and Wolfrey, C. 2013. Climate change and mental health: an exploratory case study from Rigolet, Nunatsiavut, Canada. Climatic Change, 121, 255–270.

Cunsolo Willox, A., Stephenson, E., Allen, J., Bourque, F., Drossos, A., Elgarøy, S., Kral, M.J., Mauro, I., Moses, J., Pearce, T., MacDonald, J.P., and Wexler, L. 2015. Examining relationships between climate change and mental health in the Circumpolar North. Regional Environmental Change, 15, 169–182.

de Elía, R., and Côté, H. 2010. Climate and climate change sensitivity to model configuration in the Canadian RCM over North America. Meteorologische Zeitschrift, 19, 325–339.

Derksen, C., Smith, S.L., Sharp, M., Brown, L., Howell, S., Copland, L., Mueller, D.R., Gauthier, Y., Fletcher, C.G., Tivy, A., Bernier, M., Bourgeois, J., Brown, R., Burn, C.R., Duguay, C., Kushner, P., Langlois, A., Lewkowicz, A.G., Royer A., and Walker, A. 2012. Variability and change in the Canadian cryosphere. Climatic Change, 115, 59–88.

Deshpande, B.N., Macintyre, S., Matveev, A., and Vincent, W.F. 2015. Oxygen dynamics in permafrost thaw lakes: Anaerobic bioreactors in the Canadian subarctic. Limnology and Oceanography, 60, 1656–1670.

Diaconescu, E.P., Mailhot, A., Brown, R., and Chaumont, D. 2017. Evaluation of CORDEX-Arctic

daily precipitation and temperature-based climate indices over Canadian Arctic land areas. Climate Dynamics, 50, 2061–2085.

Donat, M.G., Alexander, L.V., Yang, H., Durre, I., Vose, R., Dunn, R.J.H., Willett, K.M., Aguilar, E., Brunet, M., Caesar, J., Hewitson, B., Jack, C., Klein Tank, A.M.G., Kruger, A.C., Marengo, J., Peterson, T.C., Renom, M., Oria Rojas, C., Rusticucci, M., Salinger, J., Elrayah, A.S., Sekele, S.S., Srivastava, A.K., Trewin, B., Villarroel, C., Vincent, L.A., Zhai, P., Zhang, X., and Kitching, S. 2013. Updated analyses of temperature and precipitation extreme indices since the beginning of the twentieth century: The HadEX2 dataset. Journal of Geophysical Research: Atmospheres, 118, 2098–2118.

Du, J., Kimball, J.S., Duguay, C., Kim, Y., and Watts, J.D. 2017. Satellite microwave assessment of Northern Hemisphere lake ice phenology from 2002 to 2015. The Cryosphere, 11, 47–63.

Fauchald, P., Park, T., Tømmervik, H., Myneni, R., and Hausner, V.H. 2017. Arctic greening from warming promotes declines in caribou populations. Science Advances, 3, e1601365.

Finnis, J., and Bell, T. 2015. An analysis of recent observed climate trends and variability in Labrador. The Canadian Geographer/Le Géographe Canadien, 59, 151–166.

Ford, J.D., Pearce, T., Duerden, F., Furgal, C., and Smit, B. 2010. Climate change policy responses for Canada's Inuit population: The importance of and opportunities for adaptation. Global Environmental Change, 20, 177–191.

Ford, J.D., McDowell, G., Shirley, J., Pitre, M., Siewierski, R., Gough, W., Duerden, F., Pearce, T., Adams, P., and Statham, S. 2013. The Dynamic Multiscale Nature of Climate Change Vulnerability: An Inuit Harvesting Example. Annals of the Association of American Geographers 103, 1193–1211.

Ford, J.D., Bell, T., and Couture, N.J. 2016. Perspectives on Canada's North Coast region; in Canada's Marine Coasts in a Changing Climate, (ed.) D.S. Lemmen, F.J. Warren, T.S. James and C.S.L. Mercer Clarke. Government of Canada, Ottawa, Canada, p.153-206.

Ford, J.D., Bolton, K.C., Shirley, J., Pearce, T., Tremblay, M., and Westlake, M. 2017. Research on the Human Dimensions of Climate Change in Nunavut, Nunavik, and Nunatsiavut: A Literature Review and Gap Analysis. Arctic, 65, 289–304.

Francis, J.A., and Vavrus, S.J. 2012. Evidence linking Arctic amplification to extreme weather in mid-latitudes. Geophysical Research Letters, 39, L06801.

Francis, J.A., Vavrus, S.J., and Cohen, J. 2017. Amplified Arctic warming and mid-latitude weather: new perspectives on emerging connections. Wiley Interdisciplinary Reviews: Climate Change, 8, e474.

Fraser, R.H., Olthof, I., Carrière, M., Deschamps, A., and Pouliot, D. 2011. Detecting long-term changes to vegetation in northern Canada using the Landsat satellite image archive. Environmental Research Letters, 6, 045502.

Furgal, C., and Tremblay, M. 2010. Climate change in Nunavik: access to territory and resources. In W.F. Vincent, M. Lemay, and C. Barnard (Eds.), Impacts of environmental change in the Canadian coastal Arctic: a compendium of research conducted during ArcticNet phase 1 (2004–2008). ArcticNet, Québec City, Canada. Retrieved from http://www.arcticnet.ulaval.ca/pdf/research/compendium.pdf.

Fyfe, J.C., Boer, G.J., and Flato, G.M. 1999. The Arctic and Antarctic Oscillations and their projected changes under global warming. Geophysical Research Letters, 26, 1601-1604.

Grenier, P., de Elía, R., and Chaumont, D. 2015. Chances of short-term cooling estimated from a selection of CMIP5-based climate scenarios during 2006-35 over Canada. Journal of Climate, 28, 3232-3249.

Harper, S.L., Edge, V.L., Ford, J., Cunsolo Willox, A., Wood, M., and McEwen, S.A. 2015. Climate-sensitive health priorities in Nunatsiavut, Canada. BMC Public Health, 15, 605.

Hintze, J.L., and Nelson, R.D. 1998. Violin plots: a box plot-density trace synergism. The American Statistician, 52, 181–184.

Hu, X., and Myers, P.G. 2014. Changes to the Canadian Arctic Archipelago Sea Ice and Freshwater Fluxes in the Twenty-First Century under the Intergovernmental Panel on Climate

Change A1B Climate Scenario. Atmosphere-Ocean, 52, 331–350.

Hurrel, J.W. 2003. The North Atlantic Oscillation: Climatic Significance and Environmental Impact. American Geophysical Union. ISBN 9780875909943.

IPCC. 2013. Climate Change 2013: The Physical Science Basis. Contribution of Working Group I to the Fifth Assessment Report of the Intergovernmental Panel on Climate Change. Cambridge, United Kingdom and New York, USA. 1535p.

Jolivel, M., and Allard, M. 2017. Impact of permafrost thaw on the turbidity regime of a subarctic river: The Sheldrake River, Nunavik. Arctic Science, 3, 451–474.

Joly, S., Senneville, S., Caya, D., and Saucier, F.J. 2011. Sensitivity of Hudson Bay Sea ice and ocean climate to atmospheric temperature forcing. Climate Dynamics, 36, 1835–1849.

Ju, J., and Masek, J.G. 2016. The vegetation greenness trend in Canada and US Alaska from 1984–2012 Landsat data. Remote Sensing of Environment, 176, 1–16.

Klein Tank, A.M.G., Zwiers, F.W., Zhang, X. 2009. Guidelines on analysis of extremes in a changing climate in support of informed decisions for adaptation. Climate data and monitoring WCDMPNo. 72, WMO-TD No. 1500, pp 56. http://www.wmo.int/pages/prog/wcp/wcdmp/wcdmp_series/documents/WCDMP_72_TD_1500_en_1.pdf. Accessed May 2017.

Kobayashi, S., Ota, Y., Harada, Y., Ebita, A., Moriya, M., Onoda, H., Onogi, K., Kamahori, H., Kobayashi, C., Endo, H., Miyaoka, K., and Takahashi, K. 2015. The JRA-55 Reanalysis: General Specifications and Basic Characteristics. Journal of the Meteorological Society of Japan. Ser. II, 93, 5–48.

Krasting, J.P., Broccoli, A.J., Dixon, K.W., and Lanzante, J.R. 2013. Future changes in Northern Hemisphere snowfall. Journal of Climate, 26, 7813-7828.

Kulkarni, S., and Huang, H.-P. 2014. Changes in Surface Wind Speed over North America from CMIP5 Model Projections and Implications for Wind Energy. Advances in Meteorology, 2014, 1–10.

Laîné, A., Nakamura, H., Nishii, K., and Miyasaka, T. 2014. A diagnostic study of future evaporation changes projected in CMIP5 climate models. Climate Dynamics, 42, 2745–2761.

Langen, P.L., Brown, R., Grenier, P., Barrette, C., Chaumont, D., Derksen, C., Hamilton, J., Ingeman-Nielsen, T., Howell, S., James, T., Lavoie, D., Marchenko, S., Olsen, S.M., Rodehacke, C.B., Sharp, M., Smith, S.L., Stendel, M., and Tonboe, R.T. 2017. Baffin Bay and Davis Strait Regional Drivers of Change, Chapter 3 in Adaptation Actions for a Changing Arctic: Perspectives from the Baffin Bay-Davis Strait Region, Arctic Monitoring and Assessment Programme (AMAP), Oslo, Norway.

Leblond, M., St-Laurent, M.-H., and Côté, S.D. 2016. Caribou, water, and ice – fine-scale movements of a migratory arctic ungulate in the context of climate change. Movement Ecology, 4, 14.

Lemieux, J.-M., Fortier, R., Talbot-Poulin, M.-C., Molson, J., Therrien, R., Ouellet, M., and Murray, R. 2016. Groundwater occurrence in cold environments: examples from Nunavik, Canada. Hydrogeology Journal, 24, 1497–1513.

Lenaerts, J.T.M., van Angelen, J.H., van den Broeke, M.R., Gardner, S., Wouters B., and van Meijgaard, E. 2013. Irreversible mass loss of Canadian Arctic Archipelago glaciers. Geophysical Research Letters, 40, 870–874,

Liston, G.E., and Hiemstra, C.A. 2011. The changing cryosphere: Pan-Arctic snow trends (1979–2009). Journal of Climate, 24, 5691–5712.

Mailhot, A., and Chaumont, D. 2017. Élaboration du portrait bioclimatique futur du Nunavik – Tome I. Rapport présenté au Ministère de la Forêt, de la Faune et des Parcs. Ouranos. 216 pages. https://www.ouranos.ca/publication-scientifique/RapportNunavik2018-Tome1-Fr.pdf.

Martynov, A., Laprise, R., Sushama, L., Winger, K., Šeparović, L., and Dugas, B. 2013. Reanalysis-driven climate simulation over CORDEX North America domain using the Canadian Regional Climate Model, version 5: Model performance evaluation. Climate Dynamics, 41, 2973-3005.

Mearns, L., McGinnis, S., Korytina, D., Arritt, R., Biner, S., Bukovsky, M., Chang, H.I., Christensen, O., Herzmann, D., Jiao, Y., Kharin, S., Lazare, M., Nikulin, G., Qian, M., Scinocca, J., Winger, K., Castro, C., Frigon, A., Gutowski, W. 2017. The NA-CORDEX dataset, version 1.0. NCAR Climate Data Gateway, Boulder CO, accessed [September 2017].

Meier, W., Fetterer, F., Savoie, M., Mallory, S., Duerr, R., and Stroeve, J. 2017. NOAA/NSIDC Climate Data Record of Passive Microwave Sea Ice Concentration, Version 3. Boulder, Colorado USA. NSIDC: National Snow and Ice Data Center.

Mekis, É., and Vincent, L.A. 2011. An Overview of the Second Generation Adjusted Daily Precipitation Dataset for Trend Analysis in Canada. Atmosphere-Ocean, 49, 163–177.

Mekis, É., Vincent, L.A., Shephard, M.W., and Zhang, X. 2015. Observed trends in severe weather conditions based on humidex, wind chill, and heavy rainfall events in Canada for 1953–2012. Atmosphere-Ocean, 53, 383-397.

Milewska, E.J., Hopkinson, R.F., and Niitsoo, A. 2005. Evaluation of geo-referenced grids of 1961–1990 Canadian temperature and precipitation normals. Atmosphere-Ocean, 43, 49–75.

Mudryk, L.R., and Derksen, C. 2017. CanSISE Observation-Based Ensemble of Northern Hemisphere Terrestrial Snow Water Equivalent, Version 2. Boulder, Colorado USA. NSIDC: National Snow and Ice Data Center.

Mudryk, L.R., Derksen, C., Howell, S., Laliberté, F., Thackeray, C., Sospedra-Alfonso, R., Vionnet, V., Kushner, P.J., and Brown, R. 2018. Canadian snow and sea ice: historical trends and projections. The Cryosphere, 12, 1157-1176.

Naulier, M., Savard, M.M., Bégin, C., Gennaretti, F., Arseneault, D., Marion, J., Nicault, A., and Bégin, Y. 2015. A millennial summer temperature reconstruction for northeastern Canada using oxygen isotopes in subfossil trees. Climate of the Past, 11, 1153–1164.

Nishimura, P.H., and Laroque, C.P. 2011. Observed continentality in radial growth-climate relationships in a twelve site network in western Labrador, Canada. Dendrochronologia, 29, 17–23.

Ouranos. 2015. Vers l'Adaptation : Synthèse des connaissances sur les changements climatiques au Québec. Consortium Ouranos, Montréal, Canada, 415pp.

Overland, J.E., Dethloff, K., Francis, J.A., Hall, R.J., Hanna, E., Kim, S.J., Screen, J.A., Shepherd, T.G., and Vihma, T. 2016. Nonlinear response of mid-latitude weather to the changing Arctic. Nature Climate Change, 6, 992-999.

Pearce, T., Ford, J., Cunsolo Willox, A., and Smit, B., 2015. Inuit Traditional Ecological Knowledge (TEK) Subsistence Hunting and Adaptation to Climate Change in the Canadian Arctic. Arctic 68, 233-245.

Pedersen, R.A., Cvijanovic, I., Langen, P.L., and Vinther, B.M. 2016. The impact of regional Arctic sea ice loss on atmospheric circulation and the NAO. Journal of Climate, 29, 889-902.

Peng, G., Meier, W.N., Scott, D.J., and Savoie, M.H. 2013. A long-term and reproducible passive microwave sea ice concentration data record for climate studies and monitoring. Earth System Science Data, 5, 311–318.

Prowse, T.D., Furgal, C., Chouinard, R., Melling, H., Milburn, D., and Smith, S.L. 2009. Implications of climate change for economic development in northern Canada: Energy, resource, and transportation sectors. Ambio: A Journal of the Human Environment, 38, 272-281.

Radić, V., Bliss, A., Beedlow, A.C., Hock, R., Miles, E., and Cogley, J.G. 2014. Regional and global projections of twenty-first century glacier mass changes in response to climate scenarios from global climate models. Climate Dynamics, 42, 37-58.

Rahmstorf, S., Box, J.E., Feulner, G., Mann, M.E., Robinson, A., Rutherford, S., and Schaffernicht, E.J. 2015. Exceptional twentieth-century slowdown in Atlantic Ocean overturning circulation. Nature Climate Change, 5, 475-480.

Rapaić, M., Brown, R., Markovic, M., and Chaumont, D. 2015. An Evaluation of Temperature and Precipitation Surface-Based and Reanalysis Datasets for the Canadian Arctic, 1950–2010. Atmosphere - Ocean, 53, 283–303.

Rapinski, M., Payette, F., Sonnentag, O., Herrmann, T.M., Royer M.-J.S, Cuerrier, A., Siegwart Collier L., Hermanutz, L., Guanish, G., Elders of Kawawachikamach, Elders of Kangiqsualujjuaq,

and Elders of Nain. 2017. Listening to Inuit and Naskapi: a story of climate change supported by meteorological measurements and climate fields in eastern Subarctic Canada. Regional Environmental Change, 18, 189-203.

Richerol, T., Frechette, B., Rochon, A., and Pienitz, R. 2015. Holocene climate history of the Nunatsiavut (northern Labrador, Canada) established from pollen and dinoflagellate cyst assemblages covering the past 7000 years. The Holocene, 26, 44–60.

Riedlsperger, R. 2013. Vulnerability to changes in winter trails and travelling: A case study from Nunatsiavut. Master thesis, Memorial University of Newfoundland, Department of Geography.

Rosol, R., Powell-Hellyer, S., and Chan, L.H.M. 2016. Impacts of decline harvest of country food on nutrient intake among Inuit in Arctic Canada: Impact of climate change and possible adaptation plan. International Journal of Circumpolar Health, 75, 1–8.

Ruane, A.C., Goldberg, R., and Chryssanthacopoulos, J. 2015. Climate forcing datasets for agricultural modeling: Merged products for gap-filling and historical climate series estimation. Agricultural and Forest Meteorology, 200, 233-248.

Ruprich-Robert, Y., Msadek, R., Castruccio, F., Yeager, S., Delworth, T., and Danabasoglu, G. 2017. Assessing the Climate Impacts of the Observed Atlantic Multidecadal Variability Using the GFDL CM2.1 and NCAR CESM1 Global Coupled Models. Journal of Climate, 30, 2785–2810.

Saha, S., Moorthi, S., Pan, H.L., Wu, X., Wang, J., Nadiga, S., Tripp, P., Kistler, R., Woollen, J., Behringer, D., Liu, H., Stokes, D., Grumbine, R., Gayno, G., Wang, J., Hou, Y.-T., Chuang, H.-Y., Juang, H.-M.H., Sela, J., Iredell, M., Treadon, R., Kleist, D., Van Delst, P., Keyser, D., Derber, J., Ek, M., Meng, J., Wei, H., Yang, R., Lord, S., van den Dool, H., Kumar, A., Wang, W., Long, C., Chelliah, M., Xue, Y., Huang, B., Schemm, J.-K., Ebisuzaki, W., Lin, R., Xie, P., Chen, M., Zhou, S., Higgins, W., Zou, C.-Z., Liu, Q., Chen, Y., Han, Y., Cucurull, L., Reynolds, R.W., Rutledge G., and Goldberg, M. 2010. The NCEP climate forecast system reanalysis. Bulletin of the American Meteorological Society, 91, 1015–1057.

Saucier, F.J., Senneville, S., Prinsenberg, S., Roy, F., Smith, G., Gachon, P., Caya, D., and Laprise, R. 2004. Modelling the sea ice-ocean seasonal cycle in Hudson Bay, Foxe Basin and Hudson Strait, Canada. Climate Dynamics, 23, 303–326.

Screen, J.A., Deser, C., Smith, D.M., Zhang, X., Blackport, R., Kushner, P.J., Oudar, T., McCusker, K.E., and Sun, L. 2018. Consistency and discrepancy in the atmospheric response to Arctic sea-ice loss across climate models. Nature Geoscience, 11, 155-163.

Senneville, S., and St-Onge Drouin, S. 2013 Étude de la variation des glaces dans le système couplé océan-glace de mer de la baie d'Hudson. Rapport préparé pour le Ministère des Transports du Québec. Rimouski, Institut des sciences de la mer de Rimouski, 63 p.

Sgubin, G., Swingedouw, D., Drijfhout, S., Mary, Y., and Bennabi, A. 2017. Abrupt cooling over the North Atlantic in modern climate models. Nature communications, 8, 14375.

Sharp, M., Burgess, D.O., Cogley, J.G., Ecclestone, M., Labine, C., and Wolken, G.J. 2011. Extreme melt on Canada's Arctic ice caps in the 21st century. Geophysical Research Letters, 38, L11501.

Thompson, D.W.J., and Wallace, J.M. 1998. The Arctic oscillation signature in the wintertime geopotential height and temperature fields. Geophysical Research Letters, 25, 1297–1300.

Thornalley, D.J., Oppo, D.W., Ortega, P., Robson, J.I., Brierley, C.M., Davis, R., Hall, I.R., Moffa-Sanchez, P., Rose, N.L., Spooner, P.T., and Yashayaev, I. 2018. Anomalously weak Labrador Sea convection and Atlantic overturning during the past 150 years. Nature, 556, 227-230.

Tivy, A., Howell, S.E.L., Alt, B., McCourt, S., Chagnon, R., Crocker, G., Carrieres, T., and Yackel, J.J. 2011. Trends and variability in summer sea ice cover in the Canadian Arctic based on the Canadian Ice Service Digital Archive, 1960–2008 and 1968–2008. Journal of Geophysical Research, 116, C03007.

Trenberth, K.E., Jones, P.D., Ambenje, P., Bojariu, R., Easterling, D., Tank, A.K., Parker, D., Rahimzadeh, F., Renwick, J.A., Rusticucci, M., and Soden, B. 2007. Observations: Surface and Atmospheric Climate Change, Chap. 3 of Climate

Change 2007: The Physical Science Basis. Contribution of Working Group I to the Fourth Assessment Report of the Intergovernmental Panel on Climate Change, Solomon, S., Qin, D., Manning, M., Marquis, M., Averyt, KB, Tignor, M., Miller, HL and Chen, Z. (eds.), pp.235–336.

Vincent, L.A., and Mekis, É. 2006. Changes in daily and extreme temperature and precipitation indices for Canada over the twentieth century. Atmosphere - Ocean, 44, 177–193.

Vincent, L.A., Wang, X.L., Milewska, E.J., Wan, H., Yang, F., and Swail, V. 2012. A second generation of homogenized Canadian monthly surface air temperature for climate trend analysis. Journal of Geophysical Research: Atmospheres, 117, D18110.

Vincent, L.A., Zhang, X., Brown, R.D., Feng, Y., Mekis, E., Milewska, E.J., Wan, H., and Wang, X. L. 2015. Observed Trends in Canada's Climate and Influence of Low-Frequency Variability Modes. Journal of Climate, 28, 4545–4560.

Wan, H., Wang, X.L., and Swail, V.R. 2010. Homogenization and trend analysis of Canadian near-surface wind speeds. Journal of Climate, 22, 1209-1225.

Way, R.G., Bell, T., and Barrand, N.E. 2014. An inventory and topographic analysis of glaciers in the Torngat Mountains, northern Labrador, Canada. Journal of Glaciology, 60, 945–956.

Way, R.G., Bell, T., and Barrand, N.E. 2015. Glacier change from the early Little Ice Age to 2005 in the Torngat Mountains, northern Labrador, Canada. Geomorphology, 246, 558-569.

Way, R.G., and Lewkowicz, A.G. 2016. Modelling the spatial distribution of permafrost in Labrador–Ungava using the temperature at the top of permafrost. Canadian Journal of Earth Sciences, 53, 1010–1028.

Way, R.G., Lewkowicz, A.G., and Bonnaventure, P.P. 2017. Development of moderate-resolution gridded monthly air temperature and degree-day maps for the Labrador-Ungava region of northern Canada. International Journal of Climatology, 37, 493–508.

Way, R.G., and Viau, A.E. 2014. Natural and forced air temperature variability in the Labrador region of Canada during the past century. Theoretical and Applied Climatology, 121, 413-424.

WAVEWATCH III Development Group. 2016. User manual and system documentation of WAVEWATCH III® version 5.16, NOAA/NWS/NCEP/MMAB, Tech. Note, 329, 326 pp.

Whitaker, D. 2017. Expanded range limits of boreal birds in the Torngat Mountains of northern Labrador. Canadian Field-Naturalist, 131, 55–62.

Williams, T.D., Bennetts, L.B., Squire, V.A., Dumont D., and Bertino L. 2013. Wave-ice interactions in the marginal ice zone Part 2: Numerical implementation and sensitivity studies along 1D transects of ocean surface. Ocean Modelling, 71, 92–101,

Zamin, T.J., Côté, S.D., Tremblay, J.-P., and Grogan, P. 2017. Experimental warming alters migratory caribou forage quality. Ecological Applications, 27, 2061–2073.

Appendix A: Summary of climate indices and model simulations used in scenarios

Table A-1: Air temperature indices.

Acronym (Units)	Name	Definition
Annual mean T (°C)	Annual mean temperature	Annual average of daily mean temperature (Tmean)
DJF mean T (°C)	Winter (DJF) mean temperature	December, January and February (DJF) average of daily mean temperature (Tmean)
JJA mean T (°C)	Summer (JJA) mean temperature	June, July and August (JJA) average of daily mean temperature (Tmean)
ID (days)	Number of freezing days	Number of days with daily maximum temperature below 0 °C (Tmax <0 °C), over a winter-centered year (from July to June)
Nthaw (days)	Winter thaw events	Number of days with daily maximum temperature above 0 °C (Tmax > 0 °C) during winter period (winter period is delimited by the two dates when the 40-day centered moving average of daily mean temperature crossed -5 °C)
TDD (degree days)	Thawing Degree Days	Cumulative sum of daily mean temperature above 0 °C, over a calendar year (from January to December)
FDD (degree days)	Freezing Degree Days	Cumulative sum of daily degrees of daily mean temperature below 0 °C, over a winter-centered year (from July to June)
HDD (degree days)	Heating Degree Days	Cumulative sum of daily degrees of daily mean temperature below 17° C, over a winter-centered year (from July to June)
GDD (degree days)	Growing degree days	Cumulative sum of daily degrees of daily mean temperature above 5 °C, over a calendar year (from January to December)
SSD (calendar days)	Summer Start Day	First calendar day (from January to December) when the 10-day centered moving average of daily minimum temperature crosses the 0 °C value
SED (calendar days)	Summer End Day	First calendar day (from January to December) after August 1st, when the 10-day centered moving average of daily minimum temperature crosses the 0 °C value.
SSL (days)	Summer season length	Number of days between Summer End Day and Summer Start Day
TNn (°C)	Annual coldest temperature	Annual minimum value of daily minimum temperature
TN10 (°C)	Extreme cold nights	10^{th} percentile of daily minimum temperature over the calendar year (from January to December)
TX10 (°C)	Extreme cold days	10^{th} percentile of daily maximum temperature over the calendar year (from January to December)
TN10p (%)	Frequency of cold nights	Annual percentage of days when daily minimum temperature is smaller than the 10^{th} percentile of daily minimum temperature: Let TNij be the daily minimum temperature (Tmin) of day "i" in the year "j". Let TNi10 be the 10^{th} percentile of the Tmin for the calendar day "i" over the period of reference 1980–2004, which is computed considering a 5-day window centered on the "i" calendar day (therefore for each "i" day of the calendar, we use 25 years * 5 days = 125 data to find the percentiles corresponding to the day "i"). The TN10p index is computed as the no. of days of the year "j" where TNij < TNi10.
TX10p (%)	Frequency of cold days	Annual percentage of days when daily maximum temperature is smaller than the 10^{th} percentile of daily maximum temperature: Let TXij be the daily maximum temperature (Tmax) of day "i" in the year "j". Let TXi10 be the 10^{th} percentile of the Tmax for the calendar day "i" over

		the period of reference 1980–2004, which is computed considering a 5-day window centered on the "i" calendar day (therefore for each "i" day of the calendar, we use 25 years * 5 days = 125 data to find the percentiles corresponding to the day "i"). The TX10p index is computed as the no. of days of the year "j" where TXij < TXi10.
TXx (°C)	Annual warmest temperature	Annual maximum value of daily maximum temperature
TX90 (°C)	Extreme warm days	90th percentile of daily maximum temperature over the calendar year (from January to December)
TX90p (%)	Frequency of warm days	Annual percentage of days when daily maximum temperature is greater than the 90th percentile of daily maximum temperature: Let TXij be the daily maximum temperature (Tmax) of day "i" in the year "j". Let TXi90 be the 90th percentile of the Tmax for the calendar day "i" over the period of reference 1980–2004, which is computed considering a 5-day window centered on the "i" calendar day (therefore for each "i" day of the calendar, we use 25 years * 5 days = 125 data to find the percentiles corresponding to the day "i"). The TX90p index is computed as the no. of days of the year "j" where TXij> TXi90.
TN90p (%)	Frequency of warm nights	Annual percentage of days when daily minimum temperature is greater than the 90th percentile of daily minimum temperature: Let TNij be the daily minimum temperature (Tmin) of day "i" in the year "j". Let TNi90 be the 90th percentile of the Tmin for the calendar day "i" over the period of reference 1980–2004, which is computed considering a 5-day window centered on the "i" calendar day (therefore for each "i" day of the calendar, we use 25 years * 5 days = 125 data to find the percentiles corresponding to the day "i"). The TN90p index is computed as the no. of days of the year "j" where TNij> TNi90.

Table A-2: Precipitation indices

Acronym (Units)	Name	Definition
Annual mean Pr (mm/day)	Annual mean precipitation	Annual mean of daily precipitation
DJF mean Pr (mm/day)	Winter Mean precipitation (DJF)	December, January and February (DJF) average of daily precipitation
JJA mean Pr (mm/day)	Summer Mean precipitation (JJA)	June, July and August (JJA) average of daily precipitation
R1mm (days)	Wet days	Annual number of days with daily precipitation ≥ 1 mm/day
RX1day (mm/day)	Annual maximum 1-day precipitation	Annual maximum of daily precipitation
RX5day (mm/day)	Annual maximum 5-day precipitation	Annual maximum of 5-day accumulated precipitation
PR95 (mm/day)	95^{th} percentile of daily precipitation	95^{th} percentile of daily precipitation over all days of the year
PR99 (mm/day)	99^{th} percentile of daily precipitation	99^{th} percentile of daily precipitation over all days of the year
R95pTOT (mm)	Precipitation due to very wet days	Annual sum of daily precipitation during days with daily precipitation greater than the 95^{th} percentile of wet-day precipitation over the reference period (1980–2004)
R99pTOT (mm)	Precipitation due to extremely wet days	Annual sum of daily precipitation during days with daily precipitation greater than the 99^{th} percentile of wet-day precipitation over the reference period (1980–2004)
R95p (days)	Very wet days	Annual number of days with daily precipitation greater than the 95^{th} percentile of wet-day precipitation over the reference period (1980–2004)
R99p (days)	Extremely wet days	Annual number of days with daily precipitation greater than the 99^{th} percentile of wet-day precipitation over the reference period (1980–2004)

Table A-3: Liquid precipitation, solid precipitation and snow depth indices.

Acronym (Units)	Name	Definition
Annual mean Prsn (mm/day)	Annual mean solid precipitation	Annual mean of daily solid precipitation
Annual FRSN	Fraction of solid annual precipitation	Fraction of the total annual precipitation in the form of solid precipitation
PL1mm (days)	Number of winter rainfall	Number of days with daily liquid precipitation during the winter period (winter period is delimited by the two dates when the 40-day centered moving average of daily mean temperature crossed -5 °C)
PLTOT (mm)	Total winter rainfall	Sum of liquid precipitation during the winter period (winter period is delimited by the two dates when the 40-day centered moving average of daily mean temperature crossed -5 °C)
SDmax (m)	Maximum snow depth	Maximum snow depth during a winter-centered year (from August to July)
DSDmax (number of days from August 1st)	Date of maximum snow depth	Date of occurrence of the maximum snow depth during a winter-centered year (from August to July)
SDCSC (number of days from 1st August)	Start date of continuous snow cover	First day of the 14 consecutive-day period with snow depths ≥ 2 cm for a winter-centered year (from August to July)
EDCSC (number of days from 1st August)	End date of continuous snow cover	First day after the SDCSC, when the snow depth < 2 cm for 14 consecutive days for a winter-centered year (from August to July)
SCD (days)	Snow cover duration	Annual number of days in a winter-centered year (from August to July) with snow depths ≥ 2 cm
RX1day Snow (mm/day)	1-day maximum snowfall	Annual maximum of daily solid precipitation in a winter-centered year (from August to July)
Snow 2-year return level (mm/day)	Snow 2-year return level	Annual maximum of daily solid precipitation with 2-year return period
Snow 5-year return level (mm/day)	Snow 5-year return level	Annual maximum of daily solid precipitation with a 5-year return period
Snow 10-year return level (mm/day)	Snow 10-year return level	Annual maximum of daily solid precipitation with a 10-year return period
Snow 20-year return level (mm/day)	Snow 20-year return level	Annual maximum of daily solid precipitation with a 20-year return period

Table A-4: The RCM simulations included in the RCP 4.5 scenarios

RCM	**Simulation**	**Indices**
CCCma-CanRCM4	CCCma-CanRCM4_CanESM2_NA22	Temperature indices, Total-precipitation indices, liquid-precipitation indices, solid-precipitation indices, snow-depth indices
DMI-HIRHAM5	DMI-HIRHAM5_EC-EARTH_NA44	Temperature indices, Total-precipitation indices, liquid-precipitation indices, solid-precipitation indices, snow-depth indices
OURANOS-CRCM5	OURANOS-CRCM5_ CanESM2_NA22	Temperature indices, Total-precipitation indices, liquid-precipitation indices, solid-precipitation indices, snow-depth indices
SMHI-RCA4	SMHI-RCA4_CanESM2_NA44	Temperature indices, Total-precipitation indices, liquid-precipitation indices, solid-precipitation indices, snow-depth indices
	SMHI-RCA4_ EC-EARTH_NA44	Temperature indices, Total-precipitation indices, liquid-precipitation indices, solid-precipitation indices, snow-depth indices
UQAM-CRCM5	UQAM-CRCM5_CanESN2_NA44	Temperature indices, Total-precipitation indices, liquid-precipitation indices, solid-precipitation indices, snow-depth indices
	UQAM-CRCM5_MPI-ESM-LR_NA44	Temperature indices, Total-precipitation indices, liquid-precipitation indices, solid-precipitation indices, snow-depth indices

Table A-5: The RCM simulations included in the RCP 8.5 scenarios

RCM	Simulation	Indices
CCCma-CanRCM4	CCCma-CanRCM4_CanESM2_NA22	Temperature indices, Total-precipitation indices, liquid-precipitation indices, solid-precipitation indices, snow-depth indices
DMI-HIRHAM5	DMI-HIRHAM5_EC-EARTH_NA44	Temperature indices, Total-precipitation indices, liquid-precipitation indices, solid-precipitation indices, snow-depth indices
OURANOS-CRCM5	OURANOS-CRCM5_CanESM2ens_NA22 (ensemble of 5 simulations driven by the first 5 members of the CanESN2 ensemble)	Temperature indices, Total-precipitation indices, liquid-precipitation indices, solid-precipitation indices, snow-depth indices
SMHI-RCA4	SMHI-RCA4_CanESM2_NA44	Temperature indices, Total-precipitation indices, liquid-precipitation indices, solid-precipitation indices, snow-depth indices
	SMHI-RCA4_ EC-EARTH_NA44	Temperature indices, Total-precipitation indices, liquid-precipitation indices, solid-precipitation indices, snow-depth indices
UQAM-CRCM5	UQAM-CRCM5_CanESN2_NA44	Temperature indices, Total-precipitation indices, liquid-precipitation indices, solid-precipitation indices, snow-depth indices
	UQAM-CRCM5_MPI-ESM-MR_NA44	Temperature indices, Total-precipitation indices, liquid-precipitation indices, solid-precipitation indices, snow-depth indices
IowaState-RegCM4	IowaState-RegCM4_GFDL-ESM2M_NA22	Temperature indices, Total-precipitation indices
	IowaState-RegCM4_HadGEM2-ES_NA22	Temperature indices, Total-precipitation indices
NCAR-RegCM4	NCAR-RegCM4_MPI-M-MPI-ESM-LR_NA22	Temperature indices, Total-precipitation indices
UArizona-WRF	UArizona-WRF_GFDL-ESM2M_NA22	Temperature indices, Total-precipitation indices